Relaxation in a Jahn-Teller System. II

F. I. B. WILLIAMS* AND D. C. KRUPKA
Bell Telephone Laboratories, Murray Hill, New Jersey 07974

AND

D. P. BREEN†
University of Oxford, Clarendon Laboratory, Oxford, England

(Received 30 September 1968)

The strong-coupling model of a cubic Jahn-Teller (JT) system where a single e-type vibrational mode interacts with an E-type electronic ground state is extended to include the effects of a trigonal field, quadratic coupling, breakdown of the adiabatic approximation, and small static tetragonal-type perturbations (random strain fields in a crystal). Relaxation is treated by considering how lattice vibrations perturb an octahedral JT-active complex situated in a trigonal crystal, and it is found that spin-flip relaxation in the ground state is related to the non-spin-flip relaxation (reorientation amongst equivalent distortions) by the square of the g-tensor anisotropy of the frozen EPR spectrum and by the spin-orbit interaction within the ground state introduced by a trigonal field. The relaxation time for temperatures above the strain splittings due to random crystal strains is expected to have the form $1/\tau = aT + bT^3 + cT^5 + de^{-\Delta/kT}$, the ratio of spin-flip to non-spin-flip rates remaining constant. The magnitudes of the relaxation rates of Paper I are quite well accounted for by the model, and from those results parameters for the model are derived. There still remains some difficulty with orientation dependence of the spin-flip relaxation and with the nature of the "JT" transition" from an anisotropic to an isotropic spin-resonance spectrum.

INTRODUCTION

IN this paper we shall try to account for the relaxation results of the preceding paper[1] (henceforth referred to as I) on relaxation rates in the strongly coupled Jahn-Teller systems of octahedrally water-coordinated Cu^{2+} in $La_2Mg_3(NO_3)_{12}\cdot 24H_2O$ (LMN) and $Zn(BrO_3)_2\cdot 6H_2O$. It will be remembered that despite the similarity of the low-temperature spectrum to that for tetragonally distorted sites, the low-temperature spin-lattice relaxation rate is some four orders of magnitude faster than that for a truly static situation. That it is not a static situation is supported by the spin-echo measurements which indicate that the centers are already reorienting their distortion axis on a microsecond time scale in the region of 5°K.

The model used is again that of an isolated $Cu^{2+}:6H_2O$ octahedron of basically cubic symmetry, as has been dealt with many times before (see references in I). We follow broadly O'Brien's[2] treatment which is appropriate for the expected parameters, supplemented somewhat to include the effects of slight breakdown of the adiabatic approximation, a small trigonal field, and random strain fields. Once we have solved this isolated complex problem, we consider its coupling to the (much softer) crystalline surroundings to see how the lattice vibrations induce transition among eigenstates of the isolated complex.

The twofold degenerate E-type ground state of the copper ion (basis $|\theta\rangle$, $|\epsilon\rangle$) in an octahedral or trigonal field interacts strongly with the e-type vibrational mode of the octahedron [basis (Q_θ, Q_ϵ)]. The resulting adiabatic potential surfaces take the form of the familiar sun-warped Mexican hat of C_3 symmetry (Fig. 2 of I). The Jahn-Teller stabilization energy $E_{JT} \approx 3000$ cm^{-1} $\approx 10\times$ the e-vibrational quantum $\hbar\omega$. The adiabatic approximation is quite good and the three lowest-lying states (no radial excitation and the lowest-lying angular excitations) are a doublet nearly degenerate with a singlet lying $3\Gamma \lesssim \frac{3}{10}$ cm^{-1} above it, the closest excited states are $\gtrsim 150$ cm^{-1} higher [see Fig. 1(a)]. An E-type strain field removes the equivalence of the wells as shown in an exaggerated fashion on Fig. 1(b) leaving eigenstates $|G_x\rangle$, $|G_y\rangle$, and $|G_z\rangle$ which are predominantly localized in the well corresponding to a stretching distortion along the axis denoted by the subscript, with a small admixture $\sim\Gamma/\delta$ of the other two wells, where δ is the extent to which the wells are made nonequivalent. The width of the lines on Fig. 1(b) represents schematically $|G_i(\theta)|^2$. Intrawell phonon matrix elements $\langle G_i|\hat{O}|G_i\rangle$ dominate, indicated by wavy vertical lines on Fig. 1(b), making the transition rate between eigenstates (wells) $\propto (\Gamma/\delta)^2$. For resonant phonon transitions, however, this well decoupling is just compensated by the increase in the number of available phonons of energy δ to make this interwell (reorientation) transition rate independent of local strain and proportional to Γ^2. The measurement of the reorientation rate combined with an estimate of the coupling to the phonons is sufficient to give a value for Γ, a key parameter in the theory. In reality, of course, each of the energy levels is a Kramers doublet whose components are split by a magnetic field to give rise to the EPR signal.

The orbital contribution to the magnetic moment makes the g tensor sensitive to the distortion axis, so that each well has a distinct resonance line in general,

* Present address: D.Ph.-S.R.M., C.E.N.—Saclay, 91, Gif-sur-Yvette, France.
† Present address: College St. Albert, Leuven, Belgium.

[1] D. P. Breen, D. C. Krupka, and F. I. B. Williams, preceding paper, Phys. Rev. 179, 241 (1969).
[2] M. C. M. O'Brien, Proc. Roy. Soc. (London) A281, 323 (1964).

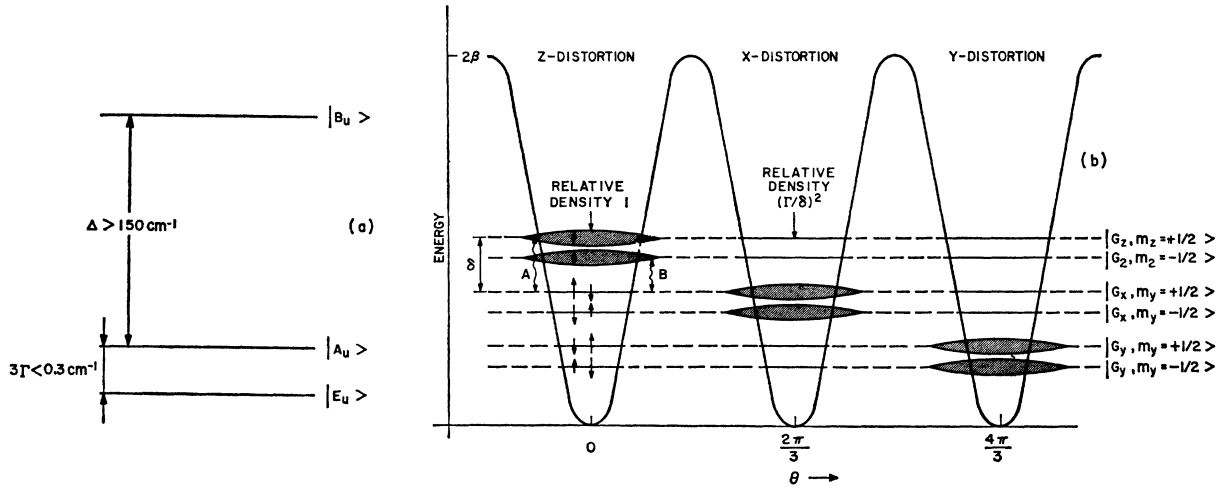

FIG. 1. (a) The four lowest-lying vibronic states for strong coupling and $\beta/\alpha \gg 1$ giving orders of magnitude of the splitting. (b) Folded-out section at constant radius $\rho = \rho_0$ through the radial minimum of the lower adiabatic potential sheet showing threefold modulation due to the nonlinear potential. The energy levels of the three lowest states are drawn for a tetragonal static strain which makes the wells inequivalent; the level widths represent schematically the wave-function amplitude $|\psi|$, δ represents the strain splitting, and the wavy lines represent the tetragonal phonon matrix elements.

its axial g-tensor ellipsoid being directed along its distortion axis. Because of this nonequivalence of g tensors, the effective spin quantization axes for a general field direction are not coincident for different wells (Fig. 2); the effective-spin part of the spin-up component $|G_x\uparrow\rangle$, say, is not in general orthogonal to the spin part of the spin-down component $|G_y\downarrow\rangle$, thereby allowing a phonon (electric-type) matrix element $\langle G_x\uparrow|\hat{O}|G_y\downarrow\rangle \neq 0$. The relaxation path to $|G_x\downarrow\rangle$ is completed by the reorientation process. $\langle G_x\uparrow|\hat{O}|G_y\downarrow\rangle$ is simply related to $\langle G_x\uparrow|\hat{O}|G_y\uparrow\rangle$ by the g tensor anisotropy, suggesting that the reorientation rate and the spin-lattice rates should be related. This mechanism is found to give quite good agreement with experiment, though there are certain difficulties with orientation dependence.

At higher temperatures, two-phonon processes become more important. These involve essentially the same electronic matrix elements discussed above, but use the whole phonon spectrum in a nonresonant way that can give rise to a T^5 temperature dependence as observed in I.

Finally, we discuss the nature of the "Jahn-Teller transition" at 38°K in LMN and conclude that reorientation is not quite fast enough to motionally narrow the line at so low a temperature and suggest that, for LMN, one may be observing the resonance from the second site which was not seen at low temperatures.

THEORY

Isolated Complex, Strong-Coupling Model

The vibronic Hamiltonian representing the interaction of the (Q_θ, Q_ϵ) vibrational modes within the (θ,ϵ) subspace of electronic functions is

$$\mathcal{H} = [E_0 + \tfrac{1}{2}\mu(P_\theta^2 + P_\epsilon^2) + \tfrac{1}{2}\mu\omega^2(Q_\theta^2 + Q_\epsilon^2) + A_3 Q_\theta(3Q_\epsilon^2 - Q_\theta^2)]I + V(Q_\theta U_\theta + Q_\epsilon U_\epsilon) + V_2[U_\theta(Q_\epsilon^2 - Q_\theta^2) + 2U_\epsilon Q_\theta Q_\epsilon], \quad (1)$$

where

$$U_\theta = \begin{pmatrix} -1 & \\ & 1 \end{pmatrix} = -\sigma_z, \quad U_\epsilon = \begin{pmatrix} & 1 \\ 1 & \end{pmatrix} = \sigma_x, \quad I = \begin{pmatrix} 1 & \\ & 1 \end{pmatrix}$$

and, for later use,

$$A_2 = \begin{pmatrix} & -i \\ i & \end{pmatrix} = \sigma_y. \quad (2)$$

Here (Q_θ, Q_ϵ) are amplitudes of e vibrations in Fig. 2 of paper I, (P_θ, P_ϵ) are momenta conjugate to (Q_θ, Q_ϵ), μ is the effective mass of the e-vibrational mode, ω is its frequency, A_3 is the coefficient describing the first-order anharmonicity of the mode, V is the reduced matrix element for linear vibronic coupling, V_2 is the reduced matrix element for quadratic vibronic coupling, and E_0 is energy in absence of distortion from cubic symmetry. The matrices are indexed in the order $(|\theta\rangle, |\epsilon\rangle)$; θ transforms as $3z^2 - r^2$, ϵ as $x^2 - y^2$. The Schrödinger equation is

$$\mathcal{H}\psi_i = E_i\psi_i, \quad (3)$$

where ψ_i is a two-component wave function

$$\begin{pmatrix} \chi_\theta^i(Q_\theta, Q_\epsilon) \\ \chi_\epsilon^i(Q_\theta, Q_\epsilon) \end{pmatrix}$$

representing a solution

$$\psi_i = \chi_\theta^i|\theta\rangle + \chi_\epsilon^i|\epsilon\rangle. \quad (4)$$

If we set

$$Q_\theta=\rho\cos\theta,\qquad Q_\epsilon=\rho\sin\theta, \tag{5}$$

and apply the unitary transformation

$$S=\begin{pmatrix}\sin\frac{1}{2}\theta & \cos\frac{1}{2}\theta\\ \cos\frac{1}{2}\theta & -\sin\frac{1}{2}\theta\end{pmatrix} \tag{6}$$

appropriate to strong coupling, we find[3,4]

$$\mathcal{H}'=S\mathcal{H}S^{-1}=\mathcal{H}_0'I-V\rho U_\theta+(\hbar^2/2\mu\rho^2)A_2 i(\partial/\partial\theta)+V_2\rho^2(\cos3\theta\,U_\theta+\sin3\theta\,U_\epsilon), \tag{7}$$

where

$$\mathcal{H}_0'=\left[E_0-\frac{\hbar^2}{2\mu\rho^2}\left(\rho\frac{\partial}{\partial\rho}\rho\frac{\partial}{\partial\rho}-\tfrac{1}{4}+\frac{\partial^2}{\partial\theta^2}\right)+\tfrac{1}{2}\mu\omega^2\rho^2-A_3\rho^3\cos3\theta\right]I.$$

Evidently if (3) is satisfied, then

$$\mathcal{H}'\varphi_i=E_i\varphi_i, \tag{8}$$

where φ_i is again a two-component wave function of (ρ,θ) and (3) is satisfied by

$$\psi_i=S^{-1}\varphi_i. \tag{9}$$

We require $\psi_i(\rho,\theta)=\psi_i(\rho,\,\theta+2\pi)$, which, because

$$S^{-1}(\theta+2\pi)=-S^{-1}(\theta),$$

dictates that

$$\varphi_i(\rho,\theta)=-\varphi_i(\rho,\,\theta+2\pi). \tag{10}$$

It might be noted that

$$\varphi=\begin{bmatrix}f\\ g\end{bmatrix}$$

represents the function

$$\varphi=(\sin\tfrac{1}{2}\theta\,|\,\theta\rangle+\cos\tfrac{1}{2}\theta\,|\,\epsilon\rangle)f+(\cos\tfrac{1}{2}\theta\,|\,\theta\rangle-\sin\tfrac{1}{2}\theta\,|\,\epsilon\rangle)g.$$

The matrix of an operator $\hat{O}$ is given by

$$\langle\psi_i|\hat{O}|\psi_j\rangle=\langle\varphi_i|S\hat{O}S^{-1}|\varphi_j\rangle. \tag{11}$$

The pair of coupled differential equations given by (8) corresponds to Eq. (10) of O'Brien[2] and to the pair (A12) of Ham.[5] The strong-coupling approximation is the neglect of the nonadiabatic (NA) terms

$$\mathcal{H}_{NA}=\frac{\hbar^2}{2\mu\rho^2}A_2 i\frac{\partial}{\partial\theta}+V_2\rho^2\sin3\theta\,U_\epsilon, \tag{12}$$

[3] This approach is essentially an amalgam of Ham's (Ref. 5) formalism for the weak-coupling limit with O'Brien's work on the strong-coupling limit. It has the advantage of providing a convenient logical framework in terms of which our ideas may be more clearly and concisely expressed.

[4] Hamiltonians in the transformed representation are primed.

[5] F. S. Ham, Phys. Rev. **166**, 307 (1968).

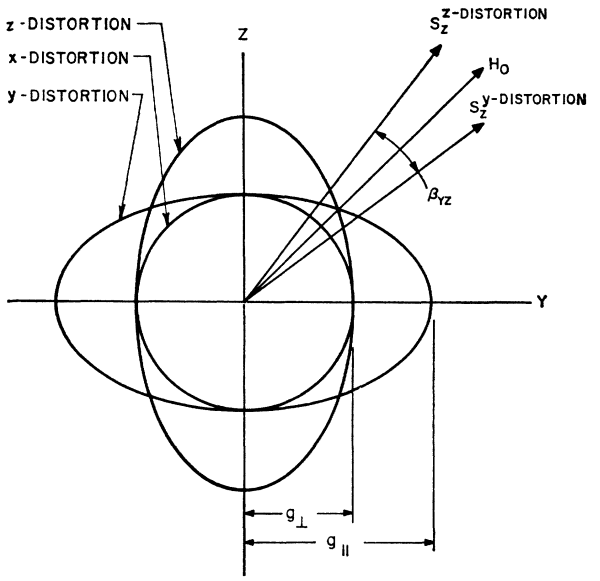

FIG. 2. g tensors and spin quantization axes for magnetic field along the [101] direction for the strain stabilized levels of Fig. (1b).

which couple the equations for the two components of φ_i. We shall treat the terms (12) by perturbation theory. For $V<0$, solutions of the form

$$\begin{bmatrix}f\\ 0\end{bmatrix}\quad\text{and}\quad\begin{bmatrix}0\\ g\end{bmatrix}$$

are appropriate to the lower and upper adiabatic potential sheets, respectively.

We shall want to add to the basic Hamiltonian the Zeeman, spin-orbit, strain, and trigonal field interactions. Once we write these down in the original representation, it is trivial to transform them since they do not involve any derivatives of the normal-mode coordinates. In the original representation, then, they are

$$\mathcal{H}_{so}=4\sigma\lambda A_2 S_\iota-(2\lambda^2/\Delta)[\tfrac{3}{4}(1-\sigma)I-\tfrac{5}{2}\sigma A_2 S_\iota], \tag{13}$$

$$\mathcal{H}(\text{Zeeman})=4\sigma\lambda A_2 h_\iota+2\mathbf{h}\cdot\mathbf{S}I-(2\lambda/\Delta)\times\{(2+\tfrac{5}{2}\lambda/\Delta+5\sigma)\mathbf{h}\cdot\mathbf{S}+(1+\tfrac{1}{2}\lambda/\Delta-\sigma)\times[(3h_zS_z-\mathbf{h}\cdot\mathbf{S})U_\theta+\sqrt{3}(h_xS_x-h_yS_y)U_\epsilon]-9\sigma h_\iota S_\iota+6\sigma[(h_\epsilon S_\epsilon-h_\theta S_\theta)U_\theta+(h_\theta S_\epsilon+h_\epsilon S_\theta)U_\epsilon]\}, \tag{14}$$

where we have assumed for simplicity that the trigonal field V_3 is caused entirely by a crystalline field acting only on the quadrupolar moment of the electronic distribution on the Cu^{2+}. Here $\sigma=(\sqrt{\frac{1}{2}})\langle E\theta\,|\,V_3\,|\,T_2\sigma\rangle/\Delta$, Δ is the cubic splitting between T_{2g} and E_g states, $\mathbf{h}=\beta\mathbf{H}$, λ is the spin-orbit coupling parameter for $3d^9\ {}^2D$, $h_\theta=(\sqrt{\frac{1}{2}})(h_x-h_y)$, $h_\epsilon=-(\sqrt{\frac{1}{6}})(2h_z-h_x-h_y)$, $h_\iota=(\sqrt{\frac{1}{3}})(h_x+h_y+h_z)$, and $S_{\theta,\epsilon,\iota}$ are similarly defined.

$$\mathcal{H}(\text{tetragonal strain})=B(e_\theta U_\theta+e_\epsilon U_\epsilon), \tag{15}$$

where $e_\theta=(\sqrt{\frac{1}{6}})(2e_{zz}-e_{xx}-e_{yy})$ and $e_\epsilon=(\sqrt{\frac{1}{2}})(e_{xx}-e_{yy})$.[6] (This expression is appropriate to an octahedron.) To write these in the transformed representation, we need only note that

$$\begin{aligned} SU_\theta S^{-1}&=-\cos\theta\, U_\theta-\sin\theta\, U_\epsilon,\\ SU_\epsilon S^{-1}&=-\sin\theta\, U_\theta+\cos\theta\, U_\epsilon,\\ SA_2S^{-1}&=-A_2. \end{aligned} \tag{16}$$

We note here the effects of a slight breakdown of the adiabatic approximation. If the zero-order solutions [i.e., solutions neglecting the terms (12)] are denoted by

$$\varphi_n{}^{(+)}=\begin{pmatrix} f_n(\rho,\theta)\\ 0\end{pmatrix}\quad \varphi_n{}^{(-)}=\begin{pmatrix} 0\\ g_n(\rho,\theta)\end{pmatrix},$$

then

$$\varphi_n{}'=\varphi_n{}^{(+)}+\sum_m \frac{\langle\varphi_m{}^{(-)}|\mathcal{H}_{NA}|\varphi_n{}^{(+)}\rangle}{E_n{}^+-E_m{}^-}\varphi_m{}^{(-)}. \tag{17}$$

We show in Appendix A that, for $\psi_n=S^{-1}\varphi_n{}'$,

$$\begin{aligned} \langle\psi_n|U_\theta|\psi_m\rangle&=\langle\varphi_n{}^{(+)}|(1+\alpha/4E_{JT})\cos\theta+(V_2\rho_0{}^2/4E_{JT})\\ &\quad\times(\cos2\theta-\cos4\theta)|\varphi_m{}^{(+)}\rangle,\\ \langle\psi_n|U_\epsilon|\psi_m\rangle&=\langle\varphi_n{}^{(+)}|(1+\alpha/4E_{JT})\sin\theta+(V_2\rho_0{}^2/4E_{JT})\\ &\quad\times(-\sin2\theta-\sin4\theta)|\varphi_m{}^{(+)}\rangle, \end{aligned} \tag{18}$$

where $\alpha=\hbar^2/2\mu\rho_0{}^2$, E_{JT} is the depth of the minimum of the trough in the adiabatic potential at $\rho=\rho_0=V/\mu\omega^2$, and $\alpha/4E_{JT}=(\hbar\omega/4E_{JT})^2$; and

$$\langle\psi_n|A_2|\psi_m\rangle=\frac{\alpha}{2E_{JT}}\langle\varphi_n{}^{(+)}|-i\frac{\partial}{\partial\theta}|\varphi_m{}^{(+)}\rangle. \tag{19}$$

Equations (16) and (18) together provide a prescription for evaluating (13)–(15) within the set of lower-sheet vibronic states.

We now turn to O'Brien's[2] work for the $\varphi_n{}^{(+)}$ solutions. She has considered the solutions appropriate to the region of the parameters estimated by Öpik and Pryce,[7] viz.,

$$\begin{aligned} E_{JT}&\approx3000\text{ cm}^{-1},\\ \hbar\omega&\approx300\text{ cm}^{-1},\\ \rho_0&=0.3\text{ Å},\\ \alpha&=\hbar^2/2\mu\rho_0{}^2\approx8\text{ cm}^{-1},\\ A_3\rho_0{}^3&\approx600\text{ cm}^{-1},\\ V_2\rho_0{}^2&\approx600\text{ cm}^{-1}. \end{aligned} \tag{20}$$

The second-order electron-vibration coupling V_2 was not estimated there, but it is reasonable to suspect that $V_2\rho^2\sim A\rho(e_\theta{}^2+e_\epsilon{}^2)^{1/2}\sim A\rho^2/\sqrt{2}R$, where R is the equilibrium ion ligand distance from which we have made the estimate above. Evidently $(\hbar\omega/E_{JT})^2\sim(\frac{1}{10})^2\ll1$, which well justifies here neglect of coupling to the upper potential sheet.

O'Brien[2] finds that the solution of (8) for the ground vibronic states may be written

$$\begin{pmatrix} f_i(\rho)\chi_n(\theta)\\ 0\end{pmatrix},$$

where $f_i(\rho)$ is a harmonic-oscillator solution in ρ of quantum $\hbar\omega$, while χ is a solution of[4]

$$\mathcal{H}_\theta{}'\chi_n(\theta)=(-\alpha\partial^2/\partial\theta^2-\beta\cos3\theta)\chi_n(\theta)=E_n\chi_n(\theta), \tag{21}$$

where

$$\alpha\approx\langle f_i(\rho)|\,\hbar^2/2\mu\rho^2|\,f_i(\rho)\rangle$$

and

$$\beta\approx\langle f_i(\rho)|\,A_3\rho^3+V_2\rho^2|\,f_i(\rho)\rangle$$

if we extend O'Brien's definition to include the second-order coupling term. Recalling the boundary condition on $\chi(\theta)$, it is convenient to classify the solutions of (21) by the irreducible representations of the group $C_{6v}=C_{3v}\times C_2$ which (21) satisfies if $\frac{1}{2}\theta$ is regarded as the variable (see Appendix B). The required solutions are those odd under C_2, for which we will use the subscript u. She argues that for $\beta\gg\alpha$ it should be possible to get good answers from linear combinations of harmonic-oscillator solutions about the minima of $\beta\cos3\theta$. From the experimental g values it is evident that $\beta>0$, i.e., the minima correspond to stretching along the octahedral axes. In a slightly recast form, O'Brien's suggestion is that if

$$\begin{aligned} |A_u\rangle&=(\sqrt{\tfrac{1}{3}})(-G_x+G_y+G_z),\\ |E_u\rangle&=(\sqrt{\tfrac{1}{6}})(2G_z+G_x-G_y),\\ |E_u'\rangle&=(\sqrt{\tfrac{1}{2}})(G_x+G_y), \end{aligned} \tag{22}$$

where $|A_u\rangle$, $|E_u\rangle$, and $|E_u'\rangle$ are the three ground-state solutions of (21), then

$$\begin{aligned} G_z&\approx(\sqrt{\tfrac{1}{2}})[f(\theta)-f(\theta-2\pi)],\\ G_x&\approx(\sqrt{\tfrac{1}{2}})[f(\theta-\tfrac{2}{3}\pi)-f(\theta-8\pi/3)],\\ G_y&\approx(\sqrt{\tfrac{1}{2}})[f(\theta-\tfrac{4}{3}\pi)-f(\theta-10\pi/3)], \end{aligned} \tag{23}$$

where $f(\theta)=(2\omega/\pi)^{1/4}e^{-\omega\theta^2}$, $\omega^2=9\beta/8\alpha$ are the harmonic-oscillator solutions, which are good zero-order solutions for $\beta\gg\alpha$. It is to be noted that $G_{x,y,z}$ are concentrated in the wells corresponding to x, y, and z axis distortions of the complex, affording an easy physical interpretation of the wave functions. To this approximation the splitting between the E_u and A_u eigenstates is given by

$$3\Gamma\approx-3(H_{zz}{}^\theta-\gamma H_{zz}{}^\theta)\approx3\beta\gamma\left[\frac{3\pi}{2}-2+\frac{3}{4}\left(\sqrt{\frac{2\alpha}{\beta}}\right)\right], \tag{24}$$

where

$$H_{ij}{}^\theta=\langle G_i|\mathcal{H}_\theta{}'|G_j\rangle,$$

$$\gamma=\langle G_z|G_x\rangle=\exp\left[-3\left(\sqrt{\frac{\beta}{2\alpha}}\right)\left(\frac{\pi}{3}\right)^2\right],$$

[6] If one identifies ligand displacements directly with the strain parameters, then $B=\sqrt{2}VR$, where R is the equilibrium ion-ligand distance; see the discussion preceding Eq. (31). $B=(\sqrt{\frac{3}{2}})V_2$ in Ham's notation (Ref. 5).

[7] U. Öpik and M. H. L. Pryce, Proc. Roy. Soc. (London) **A238**, 425 (1957).

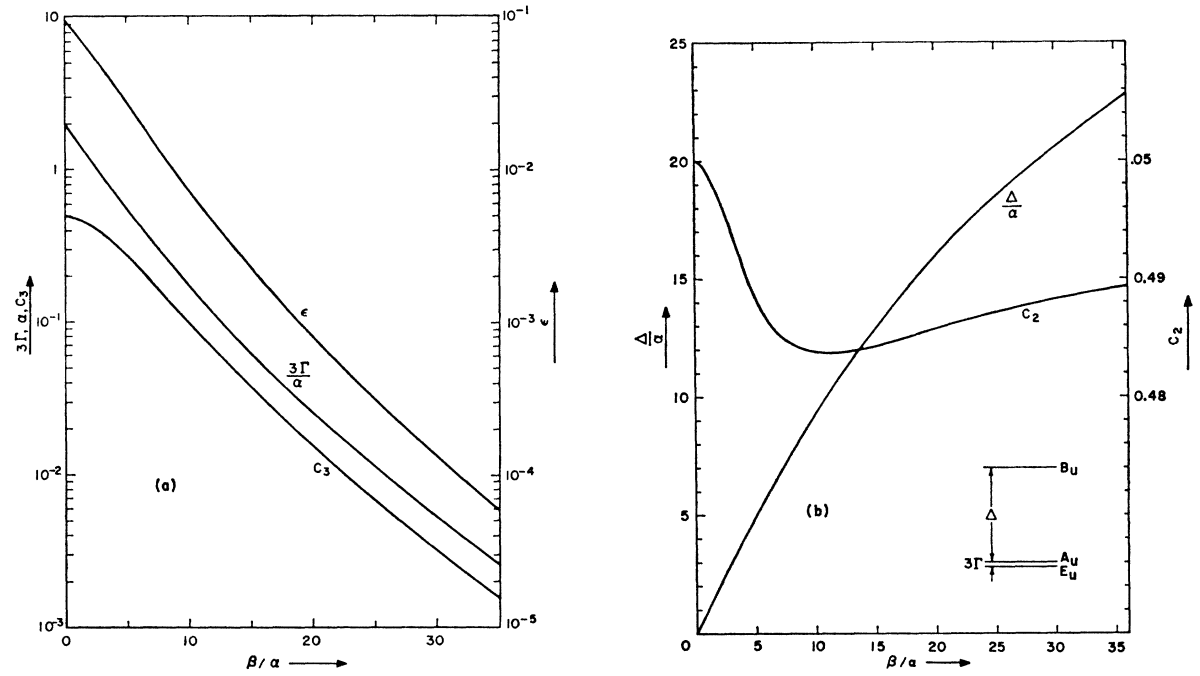

FIG. 3. Calculated parameters of ground vibronic states versus ratio of barrier half-height β to KE factor $\alpha=\hbar^2/2\mu\rho_0^2$. (a) Tunneling splitting 3Γ between ground doublet (E_u,E_u') and first excited singlet A_u, reduced matrix element for angular momentum $c_3=\langle E_u|\times\partial/\partial\theta|E_u'\rangle$ and $\epsilon=\frac{1}{3}[1-(\sqrt{\frac{1}{2}})c_1/c_2]$, where $c_1=\langle A_u|\cos\theta|E_u\rangle$ and $c_2=\langle E_u|\cos\theta|E_u\rangle$ are reduced matrix elements for $(\cos\theta, \sin\theta)$. (b) Energy difference Δ between lowest-lying B_u and A_u states and reduced matrix element c_2 for $(\cos\theta, \sin\theta)$ within ground doublet E_u. See Appendix C for details.

which gives some insight into the variation of Γ with β/α. The actual values so obtained are not as accurate as one might wish, however, due to the flattening off of the potential in the regions of $\theta=\frac{1}{3}\pi(2n+1)$, unlike true harmonic-oscillator potentials. We have computed 3Γ more exactly as outlined in Appendix C and those results are plotted in Fig. 3 together with the energy separation between the A_u level and the first level (of type B_u) above it.

O'Brien goes on to give the matrix of the Zeeman interaction in the representation (22) and calculates the g values and hyperfine constants for H along a cube axis.[8]

Random strains in the sample could, however, somewhat alter the picture and we shall sketch a theory to include both them and the trigonal field known to be present in the double nitrate crystal.[9] We shall work with the states $G_i(\theta)$ of Eq. (22) because they have a more direct physical interpretation, especially when strains are present. The matrix for $\mathcal{H}_\theta'$ is

$$\text{const } I+\begin{array}{c}\\ \langle G_x|\\ \langle G_y|\\ \langle G_z|\end{array}\begin{array}{c}\begin{array}{ccc}|G_x\rangle & |G_y\rangle & |G_z\rangle\end{array}\\ \begin{pmatrix} & -\Gamma & -\Gamma\\ -\Gamma & & \Gamma\\ -\Gamma & \Gamma & \end{pmatrix}\end{array}. \tag{25}$$

Only tetragonal (e type) strains will be important, and they are represented by an operator $\mathcal{H}_s'=\xi U_\theta+\zeta U_\epsilon$ [from Eq. (15)], where ξ and ζ are parameters which vary from site to site and can presumably be described by a statistical distribution function. The matrix of $\mathcal{H}_s'$ is

$$\mathcal{H}^{s\prime}\approx\begin{pmatrix} D_{xx} & & \\ & D_{yy} & \\ & & D_{zz}\end{pmatrix}, \tag{26}$$

where $D_{ij}\approx\langle G_i|\,\xi\cos\theta+\zeta\sin\theta\,|G_j\rangle$ $(i,j=x,y,z)$; for $i\neq j$, $D_{ij}\approx\xi\epsilon\approx\xi\gamma\ll\beta$ and we shall drop them.[8] The Zeeman interaction in this representation can be derived from (14) and (18), setting $P=\lambda/\Delta$

$$\begin{aligned}\mathcal{H}'(\text{Zeeman})=&[2-2P(2+\tfrac{5}{2}P+5\sigma)]\mathbf{h}\cdot\mathbf{S}\\ &-4PC_2(1+\tfrac{1}{2}P-\sigma)\begin{pmatrix}3h_xS_x-\mathbf{h}\cdot\mathbf{S}\\ & 3h_yS_y-\mathbf{h}\cdot\mathbf{S}\\ & & 3h_zS_z-\mathbf{h}\cdot\mathbf{S}\end{pmatrix}\\ &+6P\sigma(4C_2+3)h_iS_i-24P\sigma C_2\\ &\times\begin{pmatrix}h_xS_x+h_yS_z+h_zS_y\\ h_yS_y+h_xS_z+h_zS_x\\ h_zS_z+h_xS_y+h_yS_x\end{pmatrix},\end{aligned} \tag{27a}$$

where[10]

$$\begin{aligned}C_2=\tfrac{1}{2}\langle G_z|&\left(1+\frac{\alpha}{4E_{JT}}\right)\cos\theta\\ &+\frac{V_2\rho_0^2}{4E_{JT}}(\cos2\theta-\cos4\theta)\,|G_z\rangle,\end{aligned} \tag{27b}$$

[8] A plot of the parameter c_2 appearing in O'Brien's matrix elements may be found in Fig. 3 as well as a parameter $\epsilon=\frac{1}{3}[1-(\sqrt{\frac{1}{2}})\times c_1/c_2]$ describing the deviation of the ratio c_1/c_2 from $\sqrt{2}$. It should be remembered that the breakdown of the adiabatic approximation multiplies both c_1 and c_2 by the factor $(1+\alpha/4E_{JT})$ as shown in Appendix A.

[9] L. C. Olsen and J. W. Culvahouse, Phys. Rev. **152**, 409 (1966).

[10] In the limit $A_3=V_2=0(\beta/\alpha=0)$, C_2 is identical to Ham's q.

again neglecting the off-diagonal terms which are of order $Ph\gamma \ll \Gamma$. The remaining interaction which may be important is the spin-orbit coupling which, from (13) and (19), is

$$\mathcal{H}_{so}=\frac{-2\sigma\lambda\alpha c_3}{E_{JT}\sqrt{3}}S_i\begin{bmatrix} & i & -i \\ -i & & -i \\ i & i & \end{bmatrix}, \tag{28}$$

where $c_3=\sqrt{3}\langle G_z|\partial/\partial\theta|G_x\rangle$ is computed as described in Appendix C and plotted versus β/α in Fig. 3. Evidently if $D_{ii}-D_{jj}\gg\Gamma$,[11] the $|G_i\rangle$ are good approximate eigenfunctions, the g tensors are those appropriate to an axially distorted complex and the g tensor for $|G_z\rangle$ has principal g values, for $\sigma\ll 1$,

$$\begin{aligned} g_3^z&=2-4P(1+2C_2)(1-\tfrac{1}{2}P+\sigma)-10P^2, \\ g_1^z&=2-4P(1-C_2)(1-\tfrac{1}{2}P+\sigma)-2\sigma P-10P^2, \\ g_2^z&=2-4P(1-C_2)(1-\tfrac{1}{2}P+\sigma)+2\sigma P-10P^2. \end{aligned} \tag{29}$$

The principal axis for g_3 lies in the plane containing [001] and the trigonal axis, tilted from [001] towards [111] by an angle

$$\tan^{-1}\frac{2\sigma(3+4C_2)}{6C_2(1+\sigma)-\sigma}\approx\frac{10}{3}\sigma,$$

that for g_1 is in the same plane but perpendicular to the g_3 axis near [110] and that for g_2 lies along [$\bar{1}$10]. The g values and principal axes for $|G_x\rangle$ and $|G_y\rangle$ can be obtained by symmetry.

When $D_{ii}-D_{jj}\approx(g^i-g^j)h\approx\Gamma$, the random strains cause the resonance to smear into the region between the strain-stabilized line positions just calculated; it is to be noted, however, that the stabilizing influence of the orbital Zeeman effect takes over as $D_{ii}-D_{jj}<(g^i-g^j)h$ when $(g^i-g^j)h\gg\Gamma$, which is the regime calculated by O'Brien.[2] Whatever be the dominant anisotropic force, the $\chi(\theta)$ function will have the form

$$\chi=|G_i\rangle+\sum_{j\neq i}\alpha_{ij}|G_j\rangle/(1+\sum_{j\neq i}\alpha_{ji}^2)^{1/2}, \quad (i,j=x,y,z)$$

within which the expectation value of the Zeeman operator is

$$\frac{H_{ii}(\text{Zeeman})+\sum_{j\neq i}\alpha_{ji}^2H_{jj}(\text{Zeeman})}{1+\sum_{j\neq i}\alpha_{ji}^2}, \tag{30}$$

whose limiting values are two of H_{ii}(Zeeman), $i=x,y,z$. The spectrum will be seriously smeared only if most of the distribution of strain parameters falls within $\pm\Gamma$ and $(g_i-g_j)h\lesssim\Gamma$, for the α_{ji} are determined by the competition between the off-diagonal terms Γ and the diagonal ones H(Zeeman)+H(strain). It is interesting to note that when $g^x=g^y=g^z$,

$$\mathcal{H}_z=gh\begin{bmatrix}1 & & \\ & 1 & \\ & & 1\end{bmatrix}$$

and is invariant to any mixup caused by strains except that the selection rules are altered for zero strain—see I, Eq. (4). All this is to be found in O'Brien's[2] treatment, of course, but it is perhaps a little less obvious in her set of basis states appropriate to $\mathcal{H}'$(Zeeman)=$\mathcal{H}'$(strain)=0.

[11] The D_{ii} should really include the orbital Zeeman interaction before comparing $D_{ii}-D_{jj}$ with Γ to determine the degree of stabilization of G_i-type states.

RELAXATION

Coupling to Lattice

The coupling Hamiltonian between the lattice vibration and the complex is commonly derived by projecting the lattice modes onto the ligand positions and asserting that the ligands, accordingly displaced, impose a crystal field on the electrons through the usual first-order ligand-electron coupling. Proceeding thus, we find the following effective operators within the E subspace for the even modes of the octahedron before including the Zeeman interaction:

$$\begin{aligned} &a_{1g}\ \mathcal{H}_c(a_1)=G_6Q_{A_1}I, \\ &e_g\ \ \mathcal{H}_c(e)=G_1(Q_\theta U_\theta+Q_\epsilon U_\epsilon), \\ &t_{2g}\ \mathcal{H}_c(t_2)=2PG_2(S_xQ_\xi+S_yQ_\eta+S_zQ_\zeta)A_2, \\ &t_{1g}\ \mathcal{H}_c(t_1)=0. \end{aligned} \tag{31}$$

G_1 is the reduced matrix element for the e_g distortion mode within E_g manifold of pure electronic states. G_2 is the reduced matrix element for t_{2g} distortion mode between E_g and T_{2g} electronic states. G_6 is the reduced matrix element for a_{1g} distortion mode within E_g manifold of electronic states. These G_i are identical to those defined by Stoneham.[12] Inclusion of the Zeeman interaction gives operators with matrix element between Kramers conjugate pairs, but smaller by a factor of $\sim\beta H/\Delta$; it is these terms which are important in the spin-lattice relaxation of an isolated Kramers doublet ground state as appears in the Tutton salt,[12,13] but the relaxation rate they cause is some three to four orders of magnitude smaller than found experimentally. They are therefore ignored in what follows.[14] It is usual now to express the Q_α in strain language, viz.,

$$\begin{aligned} Q_{a1}&=\sqrt{2}Re_{a_1}=R(\sqrt{\tfrac{2}{3}})(e_{xx}+e_{yy}+e_{zz}), \\ Q_\theta&=\sqrt{2}Re_\theta=R(\sqrt{\tfrac{1}{3}})(2e_{zz}-e_{xx}-e_{yy}), \\ Q_\epsilon&=\sqrt{2}Re_\epsilon=R(e_{xx}-e_{yy}), \\ Q_\xi&=3Re_{yz},\quad Q_\eta=2Re_{xy},\quad Q_\zeta=2Re_{xy}. \end{aligned} \tag{32}$$

[12] A. M. Stoneham, Proc. Phys. Soc. (London) **85**, 107 (1965).
[13] B. Bleaney, K. D. Bowers, and D. J. E. Ingram, Proc. Roy. Soc. (London) **A228**, 147 (1955).
[14] If one wanted to include these, they would have the form noted by Stoneham for $\mathcal{H}_{direct}$, with $\mathfrak{L}_i^a$ and $\mathfrak{L}_{ij}^a$ replaced by 2×2 matrices $[\mathfrak{L}_i^a]$ and $[\mathfrak{L}_{ij}^a]$ appropriate to the total E subspace rather than for one member of it.

The strains are then expressed in terms of phonon operators with the help of the assumptions of isotropy, long wavelength, and uniformity within unit cell for the lattice vibrations as exampled by Stoneham.[12]

Such a derivation for $\mathcal{H}_c(e)$, however, is open to the objection that we have already dealt with the term $\mathcal{H}_c(e)$ in (31) in the solution of the isolated complex and so have given Q_θ and Q_ϵ the status of variables acting on the complex. We should not now treat them as parameters determined by the state of the rest of the lattice. Instead we can treat the coupling mechanism of these modes to the lattice as a modulation of the elastic potential; the phonons strain the lattice, so exerting an additional force against displacement of the Q_θ, Q_ϵ modes.[15] We show in Appendix D that such an approach yields

$$\mathcal{H}_c'(e)=\tfrac{2}{3}\sqrt{2}c_{44}R^2[e_\theta Q_\theta+e_\epsilon Q_\epsilon] \tag{33}$$

for a uniform isotropic continuous solid of shear modulus c_{44}; e_θ and e_ϵ are lattice strains due to phonons. When the $\mathcal{H}_c'(e)$ of (33) and the $\mathcal{H}_c(e)$ of (31) are transformed to the representation of Eq. (7) by the transformation S and limited to the lower sheet, they have identical forms

$$\mathcal{H}'(e)=S\mathcal{H}_cS^{-1}=B(e_\theta\cos\theta+e_\epsilon\sin\theta), \tag{34}$$

with

$$B=\sqrt{2}VR \quad \text{for (31)},$$
$$B=\tfrac{2}{3}\sqrt{2}c_{44}R^2\rho \quad \text{for (33)}.$$

We must also investigate the eigenfunctions. From (25)–(28), the zero-order eigenfunctions may be written $|im_i\rangle$, where $i\leftrightarrow x, y$, or z distortions and m_i is the spin projection quantum number $(=\pm\frac{1}{2})$ in a coordinate system $(X_iY_iZ_i)$ for the spin *which diagonalizes the Zeeman interaction* for the $|G_i\rangle$ state; the appropriate coordinate system can be easily found on noting that (27) defines a g tensor for each state $|G_i\rangle$ (see Fig. 2). The first-order eigenfunction from perturbation theory for $|G_i,m_i\rangle$ basis states are[16]

$$|im_i'\rangle=|im_i\rangle + \sum_{j\neq i}\frac{\{\Gamma_{ji}\langle m_j|m_i\rangle+\Lambda_{ji}\langle m_j|S_\iota|m_i\rangle\}}{E_{im_i}-E_{jm_j}}|jm_j\rangle, \tag{35}$$

$$\Gamma_{ji}=\Gamma\begin{bmatrix}0&-1&-1\\-1&0&1\\-1&1&0\end{bmatrix},$$

Γ as in (25). Λ_{ji} is the matrix multiplying S_ι in (28). $\langle m_j|m_i\rangle$ is the overlap integral between $S_z=m_j$ in the spin coordinate system diagonalizing $H(\text{Zeeman})_{jj}$ and $S_z=m_i$ in the system diagonalizing $H(\text{Zeeman})_{ii}$. The quantity $\langle m_j|S_\iota|m_i\rangle$ is the matrix element of S_ι between these states. If the $(X_\iota Y_iZ_i)$ system has to be rotated by Euler angles $(\alpha\beta\gamma)_{ij}$ to bring it into coincidence with the $(X_jY_jZ_j)$ system, then

$$|\langle m_j=+\tfrac{1}{2}|m_i=-\tfrac{1}{2}\rangle|^2 = |\langle m_j=-\tfrac{1}{2}|m_i=\tfrac{1}{2}\rangle|^2=\sin^2(\tfrac{1}{2}\beta_{ji});$$

in particular if the magnetic field lies along a principal axis common to both, then $\langle m_i=+\frac{1}{2}|m_j=-\frac{1}{2}\rangle=0$.

$$|\langle m_j=\pm\tfrac{1}{2}|m_i=\pm\tfrac{1}{2}\rangle|^2=\cos^2(\tfrac{1}{2}\beta_{ji})\sim 1,$$

since β_{ji} is never very large if the g tensors are not very anisotropic.

Matrix elements of $\mathcal{H}_c'(e)$ between these first-order states are (for $i\neq i$)

$$\langle jm_j'|\mathcal{H}_c(e)|im_i'\rangle=B\frac{\Lambda_{ji}\langle m_j|S_\iota|m_i\rangle+\Gamma_{ji}\langle m_j|m_i\rangle}{E_{jm_j}-E_{im_i}} \times[(C_{ii}-C_{jj})e_\theta+(S_{ii}-S_{jj})e_\epsilon], \tag{36}$$

where

$$C_{ji}=[\cos\theta]=c_2\begin{bmatrix}-1&&\\&-1&\\&&2\end{bmatrix}$$

and

$$S_{ij}=[\sin\theta]=c_2\begin{bmatrix}\sqrt{3}&&\\&-\sqrt{3}&\\&&0\end{bmatrix}$$

(the brackets indicating the matrix of the operator),

$$\langle jm_j|H_c'(t_2)|im_i\rangle = 2PG_2a_{ji}\langle m_j|S_xe_{zy}+S_ye_{zx}+S_ze_{xy}|m_i\rangle, \tag{37}$$

$$a_{ji}=(\sqrt{\tfrac{1}{3}})c_2\begin{bmatrix}0&-i&i\\i&0&i\\-i&-i&0\end{bmatrix}\frac{\alpha}{2E_{\mathrm{JT}}}.$$

The size of a typical matrix element of $\mathcal{H}_c(t_2)$ is

$$P2G_2\frac{\alpha}{2E_{\mathrm{JT}}}\langle G_x|\frac{\partial}{\partial\theta}|G_y\rangle\sim P2G_2\frac{\alpha}{E_{\mathrm{JT}}}\frac{2\pi}{3}\left(\sqrt{\frac{\beta}{\alpha}}\right)\gamma,$$

where γ is the overlap $\langle G_x|G_y\rangle$. The typical matrix element of $\mathcal{H}_c(e)$ for spin flip is

$$P(B/\delta)\Gamma\approx P(B/\delta)\beta\gamma,$$

where $\delta\approx D_{xx}-D_{yy}$. The ratio

$$\frac{\langle\uparrow|\mathcal{H}_c(t_2)|\downarrow\rangle}{\langle\uparrow|\mathcal{H}_c(e)|\downarrow\rangle}\sim\frac{4G_2}{B}\frac{\delta}{E_{\mathrm{JT}}}\sqrt{\frac{\alpha}{\beta}}\ll 1,$$

[15] We are indebted to F. S. Ham for pointing out that the philosophical objection can be reconciled by a transformation $Q\rightarrow Q+Q_0$, where Q_0 is the "phonon" displacement of the ligand; however, to obtain a value for Q_0 by the simple projection described above is still rather dubious and the approach of Appendix D, which takes into account the difference in stiffness of the hard water octahedron and the soft crystal, should give a more realistic estimate. This is a problem which occurs in all relaxation calculations in molecular crystals when the relaxing ion is protected by the hard molecule.

[16] The matrices are again indexed in the order $i=x, y, z$.

since $\delta \approx 1$ cm^{-1}, $G_2 \approx B$, and $E_{JT} \approx 3000$ cm^{-1}. We therefore neglect $H_c(t_2)$ in what follows. Making the aforementioned assumptions about the lattice vibrations, we find that the thermal average spontaneous transition rate from $|jm_j\rangle \rightarrow |im_i\rangle$ for the direct process is given by

$$W(j,m_j;\, i,m_i)_{\text{e modes}} = \mathfrak{A}u(jm_j;\, im_i)\left(\frac{E(j,m_j)-E(i,m_i)}{1-\exp\{[E(i,mj)-E(j,mi)]/kT\}}\right),$$

$$\mathfrak{A}=\frac{6(c_2B)^2}{5\pi\hbar^4 d v_T{}^5}\left[1+\frac{2}{3}\left(\frac{v_T}{v_L}\right)^5\right]. \quad (38)$$

Here d is the density, and v_L and v_T are longitudinal and transverse sound velocities, and

$$u(jm_j,im_i)=|\Lambda_{ji}\langle m_i|S_i|m_i\rangle+\Gamma_{ji}\langle m_j|m_i\rangle|^2.$$

It will be noted that for $|E_{jm_j}-E_{im_i}|\ll kT$, $W(j,m_j;\, i,m_i)$ is independent of $E(j,m_j)-E(i,m_i)$. This is a very important feature, for it ensures a single relaxation rate for all sites independent of possible random stabilization energies. The thermal average of the square of the amplitude of strain of frequency ω is $\sim(\hbar\omega/2Mv^2)\bar{n}(\omega)$, which is independent of ω when $\hbar\omega\gg kT$ ($\bar{n}$ is the Bose-Einstein number), the frequency density of lattice oscillators $\sim V(\omega^2/v^3)$, and the inter-well coupling appearing in the matrix element $\approx(\Gamma/\hbar\omega)^2$; putting these factors into Fermi's "golden rule," we see that the ω dependence due to the strain decoupling is just compensated by the increase in the density of states.

Inspection of the $u(jm_j,im_i)$ factor shows that, if Γ is the dominant term, reorientations accompanied by a spin flip ($m_i=-m_j$) are slower than simple reorientation rates ($m_i=m_j$) by $\sim\sin^2(\frac{1}{2}\beta)$. It is then convenient to divide the system into two groups of levels, a and b, corresponding to spin up and spin down, respectively. A spin-echo decay measurement on a given orientation j, say, will measure the rate of rearrangement of the system among the distortions without necessarily changing the spin orientation. The rate for this is given, for $E(j,a)-E(i,a)\ll kT$, by

$$1/\tau_j \text{ (reorientation)} = \mathfrak{A}kT\sum_i u(ja;\, ia)(1-\delta_{ij}) = 2\mathfrak{A}kT\Gamma^2, \quad \Gamma\gg\Lambda_{ji}. \quad (39)$$

The return to the equilibrium z magnetization for a given distortion will be characterized by the spin-flip rate and occurs over a time much greater than τ_j. We may then assume that each group, a or b, is in internal equilibrium during this time which is then given, as shown in Appendix E, by

$$\frac{1}{T_1}\text{ (spin lattice)} = \frac{2\mathfrak{A}kT}{3}\sum_{ij} u(ia;\, jb)(1-\delta_{ij}) = 2\mathfrak{A}kT\Gamma^2\left(\frac{g_\parallel-g_\perp}{g}\right)^2[\lambda_x{}^2\lambda_y{}^2+\lambda_y{}^2\lambda_z{}^2+\lambda_x{}^2\lambda_z{}^2], \quad (40)$$

if[17]

$$E_j{}^b-E_i{}^a\ll kT, \quad \beta_{ij}\ll 1, \quad |\Gamma\beta_{ij}|\gg|\Lambda_{ij}|^2.$$

g is the average g value and $\lambda_{x,y,z}$ are the direction cosines of the magnetic field. The independence of this relaxation time of the details of the stabilization energies results both from the special form for $W(im_i;\, jm_j)$ commented on above and from the assumption that kT is much greater than any energy differences in the system.

The phonons inducing this relaxation are of energy $E(i,a)-E(j,b)$ which may vary from site to site, obeying only some statistical distribution function it if is due to random strains; the spin energy is thus dispersed over a wide band of phonons, reducing strongly the likelihood of any phonon bottleneck effects, despite the strong coupling between spins and lattice.

As the temperature is increased, we must consider the possibility of two-phonon processes. Provided there is a direct phonon matrix element between the initial and final states, we need not invoke a third electronic level at all; the energy denominator appearing in the two-phonon transition probability is proportional to one of the phonon energies $\hbar\omega_1$ provided that $\hbar\omega_1\gg E_a-E_b$, thereby reducing the frequency dependence of the integral by 2. This brings the more familiar T^7 dependence down to T^5. This is just the process considered by Ham[5] for his Eq. (57) and, presumably, by Bersuker and Vekhter[18] for their Eq. (2).

If the two states are labeled a and b, $\langle i|\cos\theta|j\rangle\equiv C_{ij}$ and $\langle i|\sin\theta|j\rangle\equiv S_{ij}$, the two-phonon transition probability is [summing over the paths just mentioned as well as the paths involving the third ground level labeled c ($T\ll\Theta_D$)]

$$W_{a\rightarrow b}=\frac{\pi}{375}\frac{B^4k^5}{\hbar^7 d^2 v_T{}^{10}}\left[1+\frac{2}{3}\left(\frac{v_T}{v_L}\right)^5\right]^2 T^5|C_{ba}(S_{aa}-S_{bb}) +S_{ba}(C_{bb}-C_{aa})+C_{bc}S_{ca}-S_{bc}C_{ca}|^2\,\text{sec}^{-1}, \quad (41)$$

[17] Should the inequality be reversed such that $|\Lambda_{ij}|\gg\Gamma\beta$, the angular dependence would be quite different and, notably, would not have nulls along the principal axes. The factor $\Gamma^2[(g_\parallel-g_\perp)/g]^2[-]$ in (39) would be replaced by Λ^2 multiplied by a much weaker angular factor. It may seem curious to reject H_eT_2, and nonetheless retain the Λ term, but it is not difficult to show that the ratio of spin-lattice relaxation ratio caused by these two mechanisms is

$$\sim\left[2G_2P\frac{\alpha}{E_{JT}}(\sqrt{\tfrac{1}{3}})c_3\Big/\frac{B\sigma\lambda}{\delta}\frac{\alpha}{E_{JT}}(\sqrt{\tfrac{1}{3}})c_3\right]^2\approx\left(\frac{P\delta}{\sigma\lambda}\right)^2.$$

Here $P\approx\lambda/\Delta$, where Δ is the cubic field splitting making the ratio $(\delta/\sigma\Delta)^2\approx 1$ when $\sigma\approx 10^{-4}$, in which case $\Lambda_{ij}\ll\Gamma\beta$ for our regime.

[18] I. B. Bersuker and B. G. Vekhter, Fiz. Tverd. Tela 7, 1231 (1965) [English transl.: Soviet Phys.—Solid State 7, 986 (1965)].

where both phonons are e-type. To the approximation that $\epsilon=0$, the terms in $|\ \ |^2$ in (41) cancel, so that the first nonvanishing term involves the true cross matrix elements like $\langle G_x|\cos\theta|G_y\rangle\sim\epsilon$ which we neglected in calculating (36). The result for the $|\ \ |^2$ part of (41) is

$$48C_2{}^4\epsilon^2|\langle m_a|m_b\rangle|^2.$$

In view of the cancellation to order ϵ in (41), we should estimate the contribution from the Γ/δ admixtures taking into account the difference in phonon energies for the two-phonon process. Such terms are of order $(\Gamma/\delta)^2(\delta/\omega)^2$, where ω is the phonon energy and δ is the energy splitting of the two states. By introducing another ω^{-2}, the temperature dependence is reduced to T^3. The result is analogous to that obtained by Pirc, Žekš, and Gosar[19] for the O_2^- center in KCl and is, for no spin flip,

$$W_{a\to b}=\frac{6}{25\pi}\frac{(C_2B)^4\Gamma^2k^3}{\hbar^7d^2v_T{}^{10}}\left[1+\frac{2}{3}\left(\frac{v_L}{v_T}\right)^5\right]T^3 \qquad (42)$$

between any two of the states $|G_x\rangle$, $|G_y\rangle$, and $|G_z\rangle$.

If $\Lambda\ll\Gamma$, (41) and (42) taken together would indicate that the spin-lattice relaxation rate should be related to $W_{a\to b}$ without spin flip in the same way as for the direct process, indicating that the two-phonon processes contribute

$$\frac{1}{T_1}(\text{two phonon})=2(\Delta g/g)^2W(\lambda_x{}^2\lambda_y{}^2+\lambda_y{}^2\lambda_z{}^2+\lambda_z{}^2\lambda_x{}^2),$$

where

$$W=\frac{16\pi}{125}\frac{(BC_2)^2(kT)^3}{\hbar^7d^2v_T{}^{10}}\left[1+\frac{2}{3}\left(\frac{v_T}{v_L}\right)^5\right]^2\times\left((\epsilon kT)^2+\frac{15}{8\pi^2}\Gamma^2\right) \qquad (43)$$

to the spin-lattice relaxation rate.

If the splitting to the excited $|B_u\rangle$ vibronic state lies within the phonon spectrum, there is also the possibility of an Orbach-type[20] relaxation process. If the excitation energy is Δ, the Orbach process predicts a reorientation rate without spin flip:

$$\frac{1}{\tau}\approx\frac{2}{45\pi}\frac{(\alpha B)^2\Delta^3}{\hbar^4dv_T{}^5}\left[1+\frac{2}{3}\left(\frac{v_T}{v_L}\right)^5\right]\exp\left(-\frac{\Delta}{kT}\right),$$

$$\alpha=\langle E_u'|\cos\theta|B_u\rangle\approx1. \qquad (44)$$

There is a similar expression for the spin-lattice rate but containing an additional factor, similar to the $\sin^2\frac{1}{2}\beta$ described above, appropriate to the angle between the quantization axes of the ground states and the excited state. The simpler expression (44) will be sufficient for our purposes of using the nonappearance of an Orbach process to place a lower limit on Δ.

In summary, then, if $\Lambda\ll\Gamma$ we expect the non-spin-flip and the spin-flip reorientation rates to be related to one another by a factor of order $(\Delta g/g)^2$ for each of the processes considered. We expect $1/\tau$ to have the form

$$1/\tau=aT+bT^3+cT^5+de^{-\Delta/kT},$$

about which we can make a few general observations. Inspection of (43) tells us that the T^5 terms should not dominate the T^3 term until $kT\gtrsim\Gamma/6\epsilon\approx2\alpha$, noting from Fig. 3 that Γ/α and ϵ scale roughly together. bT^3 takes over from aT when

$$\frac{kT}{hc}\gtrsim\frac{(5\hbar^3dv_T{}^5)^{1/2}}{C_2B}\approx\frac{10^5}{(B/hc)(\text{cm}^{-1})}\ \text{cm}^{-1}\ \text{typically}$$

for $d=2$ g cm^{-3} and $v_T=2\times10^5$ cm sec^{-1}. It is much more difficult to predict when the exponential term might dominate, if indeed there is a vibronic level low enough to be directly excited by a phonon. The condition for the Orbach term to dominate the T^3 term is that

$$\left(\frac{\Delta}{kT}\right)^3\exp\left(-\frac{\Delta}{kT}\right)>\frac{27}{80}\frac{(B\Gamma)^2}{\hbar^3dv_T{}^5}\approx7\left(\frac{B\Gamma}{10^5}\right)^2$$

if B and Γ are each expressed in cm^{-1}. If such a temperature should turn out be to higher than $2\alpha/k$, then we should ask when the Orbach term exceeds the T^5 rate, i.e., when

$$\left(\frac{\Delta}{kT}\right)^5\exp\left(-\frac{\Delta}{kT}\right)>30\left(\frac{B\epsilon\Delta}{10^5}\right)^5$$

if B and Δ are again in cm^{-1}, and d and v_T are as assumed above.

A physical picture of the relaxation mechanisms can be quickly sketched with the aid of Figs. 1 and 2. Figure 1(a) shows the lowest-lying vibronic energy levels in the absence of strain and magnetic field; these two perturbations modify the A_u and E_u levels in the way drawn schematically in Fig. 1(b). In this figure, the thickness of the lines is intended to illustrate the relative density in that angular portion of the three-fold potential trough. The lengths of the spin arrows are drawn to indicate the relative amounts of up and down spin referred to the quantization axis appropriate to the z distortion. Wavy line A is a phonon-induced reorientation transition without spin flip, while B represents a reorientation accompanied by a spin flip. The vibronic matrix element for A will be proportional to the integral of the product of the wave-function densities at the end points of the "vertical" transition. The strength of the B transitions is this multiplied by the square of the down-spin component in $|G_x\rangle$. Figure

[19] R. Pirc, B. Žekš, and P. Gosar, J. Phys. Chem. Solids 27, 1219 (1966).
[20] R. Orbach, Proc. Roy. Soc. (London), A264, 456 (1961).

2 shows a section through the g tensors corresponding to $i=x$, y, and z; they are drawn for perfect cubic symmetry. A magnetic field direction is drawn in together with two of the quantization axes corresponding to Fig. 1.

If one chooses to view the relaxation from the point of view of the electronic parts of the wave function, one can attribute the spin relaxation to the action of the magnetic field in breaking the Kramers conjugate nature of the electronic function of $|G_i\uparrow\rangle$ to the electronic function of $|G_j\downarrow\rangle$ because of the different action of the orbital Zeeman Hamiltonian in each state. It is interesting to note that Stoneham's[12] theory for Cu^{2+} in the Tutton salt breaks down for cubic symmetry ($d=0$ in his paper) and causes the spin-lattice-relaxation expression to diverge except when H is along a principal axis. For very strong coupling, both Γ and α tend to zero, making our mechanism completely ineffective as appropriate for a static tetragonal field.

DISCUSSION

The following features of the experimental results should be accounted for. (1) The Cu^{2+} spin-resonance signal appears to originate from only one of the two inequivalent divalent metal sites in LMN; (2) g values; (3) spin-echo decay times; (4) spin-lattice relaxation time T_1: (a) magnitude, (b) angular dependence, (c) absence of bottlenecking, and (d) isotope effect; and (5) transition temperature. The portions relevant to each of these points are distinguished by the corresponding numbers.

(1) The x-ray analysis of Zalkin *et al.*[21] indicates two types of Mg:$6H_2O$ octahedra in $La_2Mg_3(NO_3)_{16}\cdot 24H_2O$, rotated from one another by 60° about a common ⟨111⟩ trigonal axis which is also the trigonal axis of the crystal. Mg(1), of site symmetry S_6, is in what would be a regular octahedron of water molecules with a Mg-O distance of 2.07 Å if the bond angles were changed by less than 1°. Mg(2) is at a site of C_3 symmetry; the Mg-O bond distances of its H_2O octahedron are also 2.07 Å but their angles deviate by up to 5° from the cubic configuration. There are twice as many Mg(2) as Mg(1) sites. The octahedral axes for sites (1) and (2) are obviously not coincident. Since these should determine the direction of the principal axes for the g tensors and there is no evidence for two noncoincident sets of g tensors, we must conclude that we are seeing a Cu^{2+} resonance from only one type of site. We shall return to this question later and concentrate for the moment on the one site we do see.

(2) The principal values of the g tensor are $g_3=2.465\pm0.001$ and $g_1=g_2=2.099\pm0.001$. Inserting these into Eq. (29), we conclude that

$$C_2=0.535\pm0.005 \tag{45}$$

and, from Eq. (27), that

$$E_{JT}/\hbar\omega\leq 1.6, \tag{46}$$

whereas the value supposed by the parameters of Öpik and Pryce[7] used by O'Brien[2] give

$$E_{JT}/\hbar\omega\approx 10.$$

It must not be forgotten, however, that Eq. (29) does not include the splitting of the T_2 state by the e vibration; this would decrease the C_2 value if the sign is as suggested by O'Brien.[2] An estimate of this effect (the value of O'Brien's Q) can be gotten from measurements on the CuK Tutton salt.[13] The environment there is nearly tetragonal (the ground state is $\cos\alpha|\epsilon\rangle+\sin\alpha|\theta\rangle$, with $\alpha=9°$), the splitting of the E state is estimated by Stoneham[6] from relaxation measurements, and the splitting of the T_2 state is gotten from the analysis of Bleaney, Bowers, and Pryce.[22] One finds

$$Q=-0.061(4PE_{JT}/\Delta).$$

The C_2 value then becomes

$$C_2=0.506\pm0.005, \tag{47}$$

which would suggest that, if $c_2=\frac{1}{2}$ and $V_2=0$,

$$E_{JT}/\hbar\omega=2.0_{-0.4}{}^{+3.0}, \tag{48}$$

which is more in keeping with the parameters of Öpik and Pryce.[7] We discuss the value of C_2 again at the end of this section.

Olsen and Culvahouse[9] have derived a value for the trigonal crystalline field for a Co^{2+} ion in the site Mg(2). Using their value and scaling according to the $\langle r^2\rangle$ integral from Co^{2+} to Cu^{2+},[23] we estimate our parameter σ in the g-value equations to be

$$\sigma\approx 0.045\pm0.010. \tag{49}$$

This should cause an anisotropy in the waist of the g tensor of

$$g_1-g_2=4P\sigma\approx 0.884\sigma=0.04,$$

which is not observed. We conclude that the EPR is due to the nearly cubic site Mg(1).

(3) The reorientation rate without spin flip as measured by spin echoes is

$$1/\tau=2\times10^5+5\times10^4T\ \text{sec}^{-1}. \tag{50}$$

If we apply Eq. (39), we find

$$1/\tau=2\Gamma^2\mathfrak{A}kT, \tag{51}$$

from which we can extract a value for Γ given the value of $\mathfrak{A}$. To get some feeling for the reliability of Γ so found, we will apply in parallel the two models proposed for the coupling constant B. By model (D) we shall mean the picture obtained by pretending that the

[21] A. Zalkin, J. D. Forrester, and D. H. Templeton, J. Chem. Phys. 39, 2881 (1963).

[22] B. Bleaney, K. D. Bowers, and M. H. L. Pryce, Proc. Roy. Soc. (London) A228, 166 (1955).

[23] R. E. Watson, M. I. T. Solid State Molecular Theory Group Technical Report No. 12, 1959 (unpublished).

deformation of the octahedron is estimated by projecting a uniform lattice wave onto the ligands to obtain their displacements. The other approach—model (T)—tries to account for the difference in stiffness between the octahedron and the rest of the crystal which is assumed to be an elastic jelly of average force constants appropriate to the low-frequency sound velocity and density, i.e., the bulk elastic constants. Thus from (34)

$$B=\sqrt{2}VR\approx 60\,000\ \text{cm}^{-1}\ \text{[model (D)]}, \tag{52a}$$

$$B=\tfrac{2}{3}\sqrt{2}R^2\rho_0 v_T{}^2 d\approx 500\ \text{cm}^{-1}\ \text{[model (T)]}, \tag{52b}$$

and, from Eq. (38),

$$\mathfrak{a}=\frac{3}{5\pi}\frac{V^2R^2}{\hbar^4 d v_T{}^5}\left[1+\frac{2}{3}\left(\frac{v_T}{v_L}\right)^5\right]\ \text{[model (D)]}, \tag{53a}$$

$$\mathfrak{a}=\frac{4}{15\pi}\frac{R^4 d\rho_0{}^2}{\hbar^4 v_T}\left[1+\frac{2}{3}\left(\frac{v_T}{v_L}\right)^5\right]\ \text{[model (T)]}. \tag{53b}$$

The density $d=2.10$ g cm^{-3}, from Zalkin *et al.*[21] From the specific-heat data of Bailey,[24] we estimate $(1/v_T{}^3)\times[1+\frac{1}{2}(v_T/v_L)^3]=0.15\times10^{-15}$ cm^{-3} sec and by assuming that $\frac{1}{2}(v_T/v_L)^2\ll1$, we take $v_T=1.84\times10^5$ cm sec^{-1}.

The values for Γ, which scale inversely with the values for B, are found to be [for models (D) and (T), respectively]

$$\Gamma\approx\ 30\ \text{MHz}=10^{-3}\ \text{cm}^{-1}, \tag{54a}$$

$$\Gamma\approx 3000\ \text{MHz}=10^{-1}\ \text{cm}^{-1}. \tag{54b}$$

Using Fig. 3 and taking a value of $\alpha=10$ cm^{-1} [see Eq. (20)] we find for β/α and Δ (the energy of the first excited vibronic state B_u) for models (D) and (T), respectively,

Γ	β/α	Δ	2β (barrier height)	
0.12×10^{-2} cm^{-1}	45	250 cm^{-1}	900 cm^{-1}	(55a)
9.0×10^{-2} cm^{-1}	20	160 cm^{-1}	400 cm^{-1}.	(55b)

The absence of any Orbach-type dependence on temperature up to 10°K indicates from (44) that

$$\frac{2}{45\pi}\frac{(\alpha B)^2 10^3 k^3}{\hbar^4 d v_T{}^5}\left(\frac{\Delta}{10k}\right)^3\exp\left(-\frac{\Delta}{10k}\right)\leq 5\times10^3\ \text{sec}^{-1}, \tag{56}$$

which reduces to [for models (D) and (T), respectively]

$$\Delta>180\ \text{cm}^{-1}, \tag{57a}$$

$$\Delta>100\ \text{cm}^{-1}. \tag{57b}$$

These are consistent with Eqs. (55).

(4a) The spin-lattice relaxation time for the most dilute (5×10^{17} Cu atoms cm^{-3}) sample measured in detail shows a linear temperature dependence up to 10°K described by

$$1/T_1\approx 100T\ \text{sec}^{-1}. \tag{58}$$

Comparison with (50) shows it to be some 500 times slower than the reorientation rate. On comparing (39) with (40),

$$R=\left(\frac{1/T_1}{1/\tau}\right)=\tfrac{2}{3}\sum_{ij}u(ia;jb)/\sum_{j\neq i}u(jb;ib). \tag{59}$$

This ratio is orientation-dependent, but its value for H along a ⟨110⟩ direction is, if $\Lambda\ll\Gamma$,

$$R=\frac{1}{4}\left(\frac{g_\parallel-g_\perp}{g}\right)^2\approx 0.7\times10^{-2}, \tag{60}$$

whereas experimentally

$$R=0.2\times10^{-2}. \tag{61}$$

The spin-lattice relaxation rate above 10°K is dominated by a T^5 contribution[1]

$$1/T_1=3\times10^{-2}T^5\ \text{sec}^{-1}\quad(T\text{ in °K}). \tag{62}$$

For the parameters (55) we calculate from Eq. (43) that, for H_0 along a ⟨110⟩ direction,

$$\begin{aligned}1/T_1&=1.5\times10^{-1}T^5\ \text{sec}^{-1}\ \text{[model (D)]},\\ 1/T_1&=1.5\times10^{-5}T^5\ \text{sec}^{-1}\ \text{[model (T)]}.\end{aligned} \tag{63}$$

It seems curious, however, that T^5 should dominate T^3 at so low a temperature. From the discussion following Eq. (44) we do not expect this to happen until $kT\gtrsim2\alpha\approx20$ cm^{-1} or 28°K. It may be that what looks like T^5 over the range $12<T<20$°K is in fact a combination of T^3 and an Orbach process due to the B_u level. The theory indicates that T^3 should begin to dominate T at $kT/hc\approx10^5/(B/hc)$, i.e., $T=3$°K, using the B of model (D) and $T=300$°K using model (T). Although the data between 12 and 20°K fit an Orbach curve with $\Delta=38$°K, the model certainly does not predict a level so low and the theoretical coefficient of such a term should be some three orders of magnitude larger than such a fit indicates. The interpretation of the T^5 term is, then, not very clear.

(4b) This is quite encouraging agreement until one considers the angular dependence. It is evident that for cubic symmetry when $\Lambda_{ij}=0$, the $u(ia,jb)=0$ when H_0 is directed along a principal axis of the octahedron for it is a principal axis of the g tensor of each distortion; there is no tip angle between quantization axes so that $\langle m_i|m_j\rangle\sim\sin\frac{1}{2}\beta=0$ for $m_i=-m_j$ for all i, j. If the magnetic field is in a (100) plane at an angle φ from a principal axis, the spin relaxation rate should vary like

$$\frac{1}{T_1}\approx\frac{1}{\tau}\frac{1}{4}\left(\frac{g_\parallel-g_\perp}{g}\right)^2\sin^2 2\varphi \tag{64}$$

[24] C. A. Bailey, Proc. Phys. Soc. (London) 83, 369 (1964).

if $\Lambda_{ij}=0$. The experimental angular dependence (Fig. 8 of I) does not show so marked a variation. The maximum rate does seem to be at about $\varphi\approx 45°$, but the ratio of maximum to minimum rate is at most a factor of 2. We note that if $\Lambda_{ij}\neq 0$, then S_i can flip spin.

As we noted earlier, a trigonal field can modify the angular dependence of $1/T_1$, notably in causing it not to vanish with H_0 along a $\langle 100\rangle$ axis. The spin-orbit coupling operator for the lower sheet introduced by the trigonal field and the incomplete decoupling of the two potential surfaces is [see Eq. (28)]

$$\Lambda_{ij}=\lambda'\sigma\begin{bmatrix} & i & -i \\ -i & & -i \\ i & i & \end{bmatrix}, \tag{65}$$

with $\lambda'=-\frac{2}{3}\sqrt{3}\lambda(\alpha/E_{JT})c_3$. For $\lambda=700$ cm^{-1}, $\alpha/E_{JT}=1/300$, and $\beta/\alpha=20$, we find $\lambda'\approx 4\times 10^{-2}$ cm^{-1}. The spectrum is apparently cubic, but due to the linewidths and the complexity of the spectrum it is unlikely that one could detect even a 2-G variation in the waist of the g tensor caused by a small trigonal field. Such a variation would correspond to $\sigma=0.012$ applying Eq. (29), suggesting that $\lambda'\sigma\leq 5\times 10^{-4}$ cm^{-1}.[17] Equation (36) would then predict that $(1/T_1)/(1/\tau)\sim(\lambda'\sigma/\Gamma)^2\leq 4\times 10^{-5}$ [for both model (D) and model (T) since c_3 and Γ scale together] for H_0 along $\langle 100\rangle$. This is still far too small, but we shall see at the end of this section that it is possible that the estimate of $\alpha/E_{JT}=1/300$ could be wrong by as much as a factor of 6, altering the ratio to 1.4×10^{-3}.

(4c) With such a rapid direct-process relaxation, one might expect a phonon bottleneck. The usual factor representing the extent of bottlenecking is $F=(C_s/C_p)\times T_{1b}/T_{s1}$, where C_s is the spin specific heat, C_p is the phonon specific heat for the heated band of phonons, T_{s1} is the spin-phonon relaxation time, and T_{1b} is the lattice-bath relaxation time. Taking $v=2\times 10^5$ cm sec^{-1}, a phonon bandwidth $\Delta\omega$ corresponding to 3-G EPR linewidth, a spin concentration N of 10^{17} cm^{-3}, and $T=4$°K,

$$\frac{C_s}{C_p}=\frac{Nh^2v^3}{2(kT)^2(\Delta\omega)}\sim 500. \tag{66}$$

If we assume $T_{1b}\sim 1$ μsec and $T_{s1}\sim 2$ msec, appropriate to our most dilute sample with 5×10^{17} cm^{-3} and 4°K, and divide the spectrum into 3×4 noncoincident lines, we find $F\sim 0.05$; bottlenecking there should not be serious. At $N\sim 2\times 10^{18}$ cm^{-3}, and $T=1.3$°K, however, $F\sim 5$, but there was again no evidence of bottleneck. This lends support to the hypothesis of stabilization by random strains which increases the band of phonons into which the spin energy is fed. A rough idea of the random strain present can be gotten from Culvahouse's[25] measurements of linewidth versus concentration for the non-Kramers rare-earth Pr^{3+} in LMN. Using Scott and Jeffries'[26] treatment of the spin-lattice interaction by the Orbach[20] approximation of using the static crystal-field parameter, Culvahouse[25] estimates the rms residual strain at zero paramagnetic concentration to be

$$\sqrt{\langle e^2\rangle_{av}}\sim 10^{-3}.$$

The model (T) lattice-orbit interaction suggests that

$$\langle(E^i-E^j)_{strain}\rangle\approx B\sqrt{\langle e^2\rangle_{av}}$$
$$\approx 40\text{ cm}^{-1}\text{ [model (D)]} \tag{67a}$$
$$\approx 0.5\text{ cm}^{-1}\text{ [model (T)]}. \tag{67b}$$

This admittedly very crude estimate makes plausible both the lack of a bottleneck and the single relaxation time ($E^i-E^j\ll kT$), at least if model (T) is more correct.

(4d) The spin-lattice relaxation rate for the protonated double nitrate was found to be some four times faster than that for the deuterated salt at the same concentration level. Although the relaxation rate is concentration-dependent, it is not so strongly so that the small difference in concentration would account for the difference in rates. The increase in rate on lightening the ligand mass has a natural explanation on our model. The only modification introduced by changing the effective mass ($\mu=20$ amu for deuterated complex, $\mu=18$ amu for the hydrated complex) is to alter the moment of inertia factor $\alpha=\hbar^2/2\mu\rho_0^2$ by 10%; from Fig. 3(a), we see that Γ^2 is increased by factors of

$$\Gamma^2(H_2O)=3\Gamma^2(D_2O)\quad\text{[model (D)]}, \tag{68a}$$
$$\Gamma^2(H_2O)=2\Gamma^2(D_2O)\quad\text{[model (T)]}, \tag{68b}$$

increasing the direct-process relaxation rate proportionately.

(5) The absence of a spectrum from site Mg(2) may be due simply to a preference of Cu^{2+} for site Mg(1), but it may also be due to a different energy-level structure. If β/α were sufficiently different for site Mg(2) that Γ or Λ would be comparable with $(g_{\parallel}-g_{\perp})\beta H$ and the random strains, the spectrum could become very strain-sensitive and the lines too broad to see [see Eq. (30)]. Such an increased value of Γ should cause more rapid reorientation and one might expect the trigonal site to show motional narrowing at a lower temperature than the cubic site.

The transition temperature for the Cu^{2+} in LMN reported by Bijl and Rose-Innes[27] with H_0 along the trigonal axis is $\Theta_{JT}\sim 38$°K.

Applying the T^5 law for T_1 at 38°K, we find $1/T_1(\Theta_{JT})\sim 2.5\times 10^7$ sec^{-1}. We expect the ratio $(1/\tau)/(1/T_1)$ to remain the same for the direct and two-phonon processes, indicating that $1/\tau(\Theta_{JT})\sim 10^9$ sec^{-1}. With H_0 along a

[25] J. W. Culvahouse (private communication); J. W. Culvahouse, L. Pfortmiller, and D. P. Schinke, J. Appl. Phys. **39**, 690 (1968).

[26] P. L. Scott and C. D. Jeffries, Phys. Rev. **127**, 32 (1962).

[27] D. Bijl and A. C. Rose-Innes, Proc. Phys. Soc. (London) **A66**, 954 (1953).

trigonal axis, the typical frequency separation is $\Delta\omega\sim 2\times 10^9$ sec^{-1}, thus only beginning to approach the motionally averaged regime, but already broadening the lines to about 50 G. The appearance of the isotropic spectrum at 38°K does not fit the motional-narrowing picture very well, but the evidence does not suggest an excited vibronic level so low, either. A possibility is that the isotropic spectrum at 40°K or so belongs to a faster relaxing-type Mg(2) site and that the cubic spectrum has become so broad from τ reorientation as not to be noticed.

That the ratio T_1/τ is preserved independent of temperature is supported by the observation[1] that, for H_0 along the [100] direction, a minimum linewidth of about 40 G occurs at $\sim$100°K; $1/T_1\sim 2.5\times 10^8$ by interpolation and applying $(g\beta/\hbar)\Delta H\approx[(g_{\parallel}-g_{\perp})\beta H/\hbar]^2\tau$ gives $1/\tau\sim 10^{-11}$ sec. The ratio $T_1/\tau\sim 400$, as observed in the direct-process region.

If one chooses to take seriously the value of C_2 given by Eq. (47), and, furthermore, assume that β arises entirely from the second-order ion-ligand electronic coupling so that $V_2\rho_0^2=\alpha$ from Eq. (21), we may use Eq. (27b) to obtain

$$\frac{E_{JT}}{\hbar\omega}=4.1\pm 0.6 \quad [\text{model (D)}]$$
$$=3.6\pm 0.6 \quad [\text{model (T)}], \qquad (69)$$

where the error estimate makes no allowance for uncertainties in Q and in the theory but reflects only the error in experimental g values.

Assuming $\hbar\omega=300$ cm^{-1}, self-consistent sets of parameters for each coupling model are found in Table I.

It might be noted that since α/E_{JT} appears in all the angular-momentum matrix elements, they are enhanced by a factor of about 6 over what we had assumed from the estimation of Öpik and Pryce. This, for example, increases by 36 the ratio $(\lambda'\sigma/\Gamma)^2$ talked about after Eq. (65) in connection with the angular variation of T_1.

Comparing the results of models (D) and (T), we believe that the latter is closer to the truth; the strain splittings of 0.5 cm^{-1} obtained from the estimated rms strain by Eq. (67) are consistent with the low-temperature linear temperature dependence of the relaxation rates. Also the value of β predicted by model (D) seems excessively high, particularly if one accepts the parameters of Table I.

Experiments with uniaxial stress could evidently provide a very stringent test of the theory. Applying stress along a ⟨110⟩ direction should leave a singlet state (z distortion) lowest and a doublet (x and y distortion) lying above it by an amount $\delta=3Bc_2e_\theta$, where e_θ in the strain resulting from the uniaxial stress. This should lead to a redistribution of population in these states and hence a relative intensity variation in their ESR lines from which a value for B may be obtained directly. In addition, the relaxation rates (both $1/\tau$ and $1/T_1$) in these states should change with δ as

$$\delta/(e^{+\delta/kT}-1).$$

Unfortunately, the double nitrate is a very fragile crystal and it might break before sufficiently high stresses can be applied, but it should be possible with harder crystals, e.g., for Cu^{2+} in CaO,[28] MgO,[29,30] or $KZnF_3$.[31]

TABLE I. Self-consistent sets of parameters for each coupling model.

Parameter	Model (D) (cm^{-1})	Model (T) (cm^{-1})
Γ	10^{-3}	10^{-1}
E_{JT}	1250	1100
α	18	20
β	810	450
$E(B_u)-E(A_u)$	1000	360

CONCLUSIONS

We have been able to account reasonably successfully for the spin-lattice and reorientation relaxation rates for Cu^{2+} in $La_2Mg_3(NO_5)_{12}\cdot 24H_2O$ as measured in I by developing somewhat the basic model proposed by Van Vleck[32] and elaborated on by Öpik and Pryce[7] and O'Brien.[2] The model is a $Cu^{2+}\cdot 6H_2O$ octahedron, with linear and quadratic ion-ligand coupling and some elastic anharmonicity, perturbed by the phonons of the crystal in which it is embedded. The phonons induce relaxation between those lowest-lying spin-vibronic levels which give rise to the spin-resonance signal by both resonant (one phonon) and nonresonant (two phonon) processes. We found that the reorientation relaxation rate is directly related to the "tunneling" parameter, similar to what Pirc, Žekš, and Gosar[19] found for the reorientation of the O_2^- center in KCl, which they called phonon-assisted tunneling. We concluded that the spin-lattice relaxation was really a two-step process wherein the complex undergoes a simultaneous spin flip and reorientation followed by a simple reorientation without spin flip. The ratio of the spin-flip rate to the non-spin-flip rate was found to be approximately the square of the low-temperature (frozen spectrum) g-tensor anisotropy, independent of whether one- or two-phonon processes dominated. The model's success can be judged by the reasonableness of the parameters (Table I) required to fit the experimental data. However, the model has not accounted con-

[28] W. Low and J. T. Suss, Phys. Letters 7, 310 (1963).
[29] J. W. Orton, P. Auzins, J. H. E. Griffiths, and J. E. Wertz, Proc. Phys. Soc. (London) 78, 554 (1961).
[30] R. E. Coffman, J. Chem. Phys. 48, 609 (1968).
[31] F. I. B. Williams, F. R. Merritt, and H. Guggenheim (unpublished).
[32] J. H. Van Vleck, J. Chem. Phys. 7, 72 (1939).

vincingly for the angular dependence of the spin-lattice relaxation rate or for the transition temperature to an isotropic spectrum, although possible means of reconciliation have been proposed in each case.

ACKNOWLEDGMENTS

We are especially grateful for the fruitful discussions with Frank S. Ham and Mary C. M. O'Brien. We should also like to thank Professor B. Bleaney for extending the facilites of the Clarendon Laboratory, Oxford, where this work was begun during D. C. Krupka's tenure of a National Research Council of Canada Postdoctoral Fellowship and F. I. B. Williams' tenure of an Associated Electrical Industries, Ltd., Fellowship in Physics at the University of Oxford.

APPENDIX A: BREAKDOWN OF ADIABATIC APPROXIMATION

Working in the representation of Eq. (7), we shall label the solutions before consideration of $\mathcal{H}_{NA}$ of Eq. (12) as

$$\varphi_n^+(0)=\begin{pmatrix} f_n(\rho,\theta) \\ 0 \end{pmatrix},\quad \varphi_m^-(0)=\begin{pmatrix} 0 \\ g_m(\rho,\theta) \end{pmatrix}.$$

Here n and m are quantum numbers distinguishing solutions. The energies of the upper- and lower-sheet solutions are E_m^- and E_n^+, respectively; for g and f concentrated around ρ_0, $E_{nm}^- - E_{nm}^+ \sim 4E_{JT}$. The first-order wave functions for the lower sheet are seen to be

$$|\varphi_n^{+\prime}\rangle = |f_n\rangle\begin{bmatrix}1\\0\end{bmatrix}+\sum_m \left(\langle g_m|[01]\mathcal{H}_{NA}\begin{bmatrix}1\\0\end{bmatrix}|f_n\rangle \Big/ (E_n^+ - E_m^-)\right)\begin{bmatrix}0\\1\end{bmatrix}|g_m\rangle. \quad \text{(A1)}$$

Now

$$[01]\mathcal{H}_{NA}\begin{bmatrix}1\\0\end{bmatrix} = -\alpha\frac{\partial}{\partial\theta}+V_2\rho^2\sin3\theta,$$

and noting that

$$\langle g_m|-\alpha(\partial/\partial\theta)|f_n\rangle^* = \langle f_n|\alpha(\partial/\partial\theta)|g_m\rangle,$$

we can write

$$\langle\varphi_n^{+\prime}| = \langle f_{n'}|[10] + \sum_m \frac{\langle f_{n'}|\alpha(\partial/\partial\theta)+V_2\rho^2\sin3\theta|g_m\rangle}{E_{n'}^+ - E_m^-}\langle g_m|[01]. \quad \text{(A2)}$$

We can write the matrix element of an operator

$$\hat{O}=\hat{O}(\rho,\theta)\sigma,$$

where σ is a general 2×2 matrix as

$$\langle\varphi_{n'}^{+\prime}|\hat{O}|\varphi_n^{+\prime}\rangle = \langle f_{n'}|[10]\sigma\begin{bmatrix}1\\0\end{bmatrix}\hat{O}|f_n\rangle - \sum_m \frac{1}{E_n^+ - E_m^-} \times\Big\{\langle f_{n'}|[10]\sigma\begin{bmatrix}0\\1\end{bmatrix}\hat{O}|g_m\rangle\langle g_m|\alpha\frac{\partial}{\partial\theta}-V_2\rho^2\sin3\theta|f_n\rangle + \langle f_{n'}|-\alpha(\partial/\partial\theta)-V_2\rho^2\sin3\theta|g_m\rangle \times\langle g_m|[01]\sigma\begin{bmatrix}1\\0\end{bmatrix}\hat{O}|f_n\rangle\Big\}. \quad \text{(A3)}$$

If we restrict f_n and $f_{n'}$ to the lowest-lying solutions, they are quite localized in ρ about ρ_0, so that if $\hat{O}$ is a suitably well-behaved operator, the state $|g_m\rangle$ to which the matrix elements are appreciable will be similarly concentrated around $\rho=\rho_0$ with energies all about $4E_{JT}$ above

$$f_n\begin{bmatrix}1\\0\end{bmatrix};$$

the energy denominator may then be replaced by $-4E_{JT}$ and closure applied to the $\sum_m |g_m\rangle\langle g_m|$ to give

$$\begin{aligned}\langle\varphi_{n'}^{+\prime}|\hat{O}|\varphi_n^{+\prime}\rangle \approx{}& \langle f_{n'}|[10]\sigma\begin{bmatrix}0\\1\end{bmatrix}\hat{O}|f_n\rangle + \frac{1}{4E_{JT}} \times\langle f_{n'}|[10]\sigma\begin{bmatrix}0\\1\end{bmatrix}\hat{O}\left(\alpha\frac{\partial}{\partial\theta}-V_2\rho^2\sin3\theta\right) \\ &-[01]\sigma\begin{bmatrix}1\\0\end{bmatrix}\left(\alpha\frac{\partial}{\partial\theta}+V_2^2\sin3\theta\right)\hat{O}|f_n\rangle \\ ={}& \langle f_{n'}|\hat{O}|f_n\rangle \qquad \text{for } \sigma=I \\ ={}& -\langle f_{n'}|\hat{O}|f_n\rangle \qquad \text{for } \sigma=U_\theta \\ \approx{}& \langle f_{n'}|\frac{+i\alpha}{4E_{JT}} \times\left(\hat{O}\frac{\partial}{\partial\theta}+\frac{\partial}{\partial\theta}\hat{O}-V_2[\hat{O},\rho^2\sin3\theta]\right)|f_n\rangle \\ &\qquad \text{for } \sigma=A_2 \\ \approx{}& \langle f_{n'}|\frac{\alpha}{4E_{JT}}\left(\left[\hat{O},\frac{\partial}{\partial\theta}\right]-V_2\rho^2\sin3\theta\hat{O} - V_2\hat{O}\rho^2\sin3\theta\right) \quad \text{for } \sigma=U_\epsilon. \end{aligned} \quad \text{(A4)}$$

Noting that

$$[\sin\theta,\partial/\partial\theta]=-\cos\theta,$$
$$[\cos\theta,\partial/\partial\theta]=\sin\theta,$$

we see that the matrix elements for $SU_\theta S^{-1}=-\cos\theta U_\theta$

$-\sin\theta U_\epsilon$ of Eq. (16) are

$$\langle f_{n'}|\cos\theta\left(1+\frac{\alpha}{4E_{JT}}\right)+\frac{V_2\rho_0^2}{4E_{JT}}(\cos2\theta-\cos4\theta)|f_n\rangle, \quad \text{(A5)}$$

those of

$$SU_\epsilon S^{-1}=-\sin\theta\, U_\theta+\cos\theta\, U_\epsilon$$

are

$$\langle f_{n'}|\sin\theta\left(1+\frac{\alpha}{4E_{JT}}\right)+\frac{V_2\rho_0^2}{4E_{JT}}(-\sin2\theta-\sin4\theta)|f_n\rangle, \quad \text{(A6)}$$

and those of

$$SA_2S^{-1}=-A_2$$

are

$$\langle f_{n'}|-\frac{i\alpha}{2E_{JT}}\frac{\partial}{\partial\theta}|f_n\rangle. \quad \text{(A7)}$$

If we choose for the function f_n the ground-state solution for no warp $f_1=\cos\frac{1}{2}\theta$ and $f_2=\sin\frac{1}{2}\theta$, then

$$\begin{aligned}&\langle f_1|SU_\theta S^{-1}|f_1\rangle=\tfrac{1}{2}(1+\alpha/4E_{JT}),\\&\langle f_1|SU_\epsilon S^{-1}|f_2\rangle=\tfrac{1}{2}(1+\alpha/4E_{JT}),\\&\langle f_1|SA_2S^{-1}|f_2\rangle=-i\alpha/4E_{JT}.\end{aligned} \quad \text{(A8)}$$

The factors p and q defined by Ham[5] are then seen to be

$$\begin{aligned}&q=\tfrac{1}{2}(1+\alpha/4E_{JT})=\tfrac{1}{2}[1+(\hbar\omega/4E_{JT})^2],\\&p=\alpha/4E_{JT}=(\hbar\omega/4E_{JT})^2,\end{aligned} \quad \text{(A9)}$$

which satisfy the relationship $q=\frac{1}{2}(1+p)$.

Recalling that the solutions f_n can be classified according to the irreducible representations (IR) of C_{6v} as outlined in Appendix B, we note that each of the pairs $(\cos\theta, \sin\theta)$, $(\cos2\theta, -\sin2\theta)$, and $(\cos4\theta, \sin4\theta)$ forms a basis for the E_g IR of C_{6v} transforming in the same way. We can then write (A5) as

$$C(\Gamma,\Gamma')\langle f_{\Gamma,\mu}|\cos\theta|f_{\Gamma',\mu'}\rangle$$

and (A6) as

$$C(\Gamma,\Gamma')\langle f_{\Gamma,\mu}|\sin\theta|f_{\Gamma',\mu'}\rangle.$$

$C(\Gamma,\Gamma')$ is essentially a correction factor for the matrix elements of $SU_\theta S^{-1}$ and $SU_\epsilon S^{-1}$ due to the breakdown of the adiabatic approximation. If one uses linear combinations of harmonic oscillators for the E_u and A_u ground states following O'Brien, it can be shown that for $\gamma\ll1$ and $V_c\rho_0^2/4E_{JT}\ll1$

$$C(E_u,E_u)=C(E_u,A_u)\approx(1+\alpha/4E_{JT}). \quad \text{(A10)}$$

(The matrix elements for $\cos2\theta$ and $-\cos4\theta$ cancel to first order.) Still in this approximation, then the c_1 and c_2 of O'Brien are modified to C_1 and C_2, where

$$\frac{C_1}{C_2}=\sqrt{2}, \quad C_2=\frac{1}{2}\left(1+\frac{\alpha}{4E_{JT}}\right)\left(1-\frac{1}{8w}\right), \quad \text{(A11)}$$

where $w=\frac{3}{2}(\beta/2\alpha)^{1/2}$. This is the C_2 appropriate to Eq. (27).

APPENDIX B: CLASSIFICATION OF VIBRONIC STATES

Equation (21) may be written in terms of the angle $\varphi=\frac{1}{2}\theta$ to become

$$\left(-\frac{1}{4}\frac{\hbar}{2\mu\rho^2}\frac{\partial^2}{\partial\varphi^2}-\beta\cos6\varphi\right)\chi(\varphi)=E\chi(\varphi). \quad \text{(B1)}$$

It evidently satisfies the point group C_{6v}. The boundary conditions of Eq. (10) require that $\chi(\varphi)=\chi(\varphi+2\pi)$, and $\chi(\varphi)=-\chi(\varphi+\pi)$. We note that

$$C_{6v}=C_{3v}\times C_2, \quad C_2^2=I, \quad C_2G=GC_2,$$

for all members G of the group so that the IR's of C_{6v} may be divided into two sets—those even under C_2 and those odd under C_2. It is the latter that are the required solutions of (1). To make the application of C_{6v} to our problem more evident, we shall rearrange the character table of C_{6v} from its usual form and relabel the IR's. See Table II. We have chosen as standard sets of bases for the E IR's

$$\begin{pmatrix}E_g\\E_{g'}\end{pmatrix}\leftrightarrow\begin{pmatrix}\cos2\varphi\\\sin2\varphi\end{pmatrix}=\begin{pmatrix}\cos\theta\\\sin\theta\end{pmatrix}, \quad \text{(B2)}$$

$$\begin{pmatrix}E_u\\E_{u'}\end{pmatrix}\leftrightarrow\begin{pmatrix}\cos\varphi\\\sin\varphi\end{pmatrix}=\begin{pmatrix}\cos\frac{1}{2}\theta\\\sin\frac{1}{2}\theta\end{pmatrix}. \quad \text{(B3)}$$

Some other basis function pairs transforming in this standard way are

$$E_g\begin{pmatrix}\cos(3n+1)\theta\\\sin(3n+1)\theta\end{pmatrix}, \quad \begin{pmatrix}\cos(3n+2)\theta\\-\sin(3n+2)\theta\end{pmatrix} \quad n=0,1,2,3,\cdots \quad \text{(B4)}$$

$$E_u\begin{pmatrix}\cos(3n+\frac{1}{2})\theta\\\sin(3n+\frac{1}{2})\theta\end{pmatrix}, \quad \begin{pmatrix}\cos(3n+\frac{5}{2})\theta\\-\sin(3n+\frac{5}{2})\theta\end{pmatrix} \quad n=0,1,2,3,\cdots. \quad \text{(B5)}$$

TABLE II. Rearrangement of character table of C_{6v}. The IR's are relabeled, and $n=1, 2, 3, \cdots$.

Usual labels	Our labels	E	$2C_3$	$3\sigma_v$	C_2	$2C_6$	$3\sigma_v'$	Sample bases
A_1	A_g	1	1	1	1	1	1	$\cos6n\varphi$
A_2	B_g	1	1	−1	1	1	−1	$\sin6n\varphi$
E_2	E_g	2	−1	0	2	−1	0	
B_2	A_u	1	1	1	−1	−1	−1	$\cos3n\varphi$
B_1	B_u	1	1	−1	−1	−1	1	$\sin3n\varphi$
E_1	E_u	2	−1	0	−2	1	0	

APPENDIX C: COMPUTATION OF MATRIX ELEMENTS BETWEEN GROUND VIBRONIC STATES

We wish to solve the eigenvalue problem

$$\left[\frac{\partial^2}{\partial\theta^2}+\left(\frac{E}{\alpha}+\frac{\beta}{\alpha}\cos 3\theta\right)\right]\psi(\theta)=0, \tag{C1}$$
$$\psi(\theta)=-\psi(\theta+\pi)=\psi(\theta+2\pi),$$

for its lowest-lying eigenstates and to compute the matrices of $\cos\theta$, $\sin\theta$, and $\partial/\partial\theta$ within these states.

As discussed in Appendix B, the solutions may be classified according to the IR's of the point group C_{6v}. In the notation of Appendix B, the solutions which will particularly interest us are the lowest-lying state of each type E_u, A_u and B_u.

Consider the manifold spanned by $|E_u\rangle$, $|E_u'\rangle$, and $|A_u\rangle$ and define states $|G_x\rangle$, $|G_y\rangle$, and $|G_z\rangle$ by the orthogonal transformation

$$\begin{bmatrix}A_u\\E_u\\E_u'\end{bmatrix}=\begin{bmatrix}\sqrt{\frac{1}{3}} & \sqrt{\frac{1}{3}} & \sqrt{\frac{1}{3}}\\ \sqrt{\frac{1}{6}} & -\sqrt{\frac{1}{6}} & \sqrt{\frac{2}{3}}\\ \sqrt{\frac{1}{2}} & \sqrt{\frac{1}{2}} & 0\end{bmatrix}\begin{bmatrix}G_x\\G_y\\G_z\end{bmatrix}, \tag{C2}$$

or, symbolically, $U=SX$, $SS^T=I$. If the matrix of an operator $\hat{m}$ in the U representation is M, its matrix in the X representation in M' is S^TMS. It is easily shown (Ref. 2) that if

$$\hat{m}=\cos\theta,\quad M=\begin{bmatrix}&c_1&\\c_1&c_2&\\&&-c_2\end{bmatrix},$$
$$M'=c_2\begin{bmatrix}-1+2\epsilon & -2\epsilon & \epsilon\\ -2\epsilon & -1+2\epsilon & -\epsilon\\ \epsilon & -\epsilon & 2-4\epsilon\end{bmatrix};$$
$$\hat{m}=\sin\theta,\quad M=\begin{bmatrix}&&-c_1\\&&c_2\\-c_1&c_2&\end{bmatrix},$$
$$M'=\sqrt{3}c_2\begin{bmatrix}1-2\epsilon & & \epsilon\\ & -1+2\epsilon & \epsilon\\ \epsilon & \epsilon & \end{bmatrix}; \tag{C3}$$
$$\hat{m}=\partial/\partial\theta,\quad M=\begin{bmatrix}&c_3&\\-c_3&&\end{bmatrix},$$
$$M'=(\sqrt{\tfrac{1}{3}})c_3\begin{bmatrix}&1&-1\\-1&&-1\\1&1&\end{bmatrix};$$
$$\hat{m}=\alpha(\partial^2/\partial\theta^2)+\beta\cos 3\theta,\quad M=\Gamma\begin{bmatrix}2&&\\&-1&\\&&-1\end{bmatrix},$$
$$M'=\Gamma\begin{bmatrix}&-1&-1\\-1&&1\\-1&1&\end{bmatrix},$$

where ϵ is defined by $c_1/c_2=\sqrt{2}(1-3\epsilon)$. The states $|G_x\rangle$, $|G_y\rangle$, and $|G_z\rangle$ correspond very closely to the states

$$(\sqrt{\tfrac{1}{2}})[f(\theta-\tfrac{4}{3}\pi)-f(\theta-10\pi/3)],$$
$$(\sqrt{\tfrac{1}{2}})[f(\theta-\tfrac{2}{3}\pi)-f(\theta-8\pi/3)], \tag{C4}$$

and

$$(\sqrt{\tfrac{1}{2}})[f(\theta)-f(\theta-2\pi)],$$

described by O'Brien's Eq. (27) in the limit of small overlap; the convenience of the G_x, G_y, G_z representation lies in their orthonormality.

O'Brien has suggested that, for deep wells $\beta/\alpha\gg 1$; it should be a good approximation to the states A, E, and E' to assume the $|G_x\rangle$, $|G_y\rangle$, and $|G_z\rangle$ states to be those appropriate to harmonic-oscillator potentials centered on $\theta=\frac{2}{3}\pi$, $\frac{4}{3}\pi$, and 0, respectively. However, the fact that the potential flattens off between the wells suggests that the decay of $f(\theta)$ functions should be less fast than suggested by the harmonic-oscillator approximation and matrix elements sensitive to this region of the wave function—those for Γ and $\partial/\partial\theta$—may not be well approximated. Indeed, a WKB solution for $\beta/\alpha\gg 1$ in the region near the $\theta=\frac{1}{3}\pi(2n+1)$ approximates the form $(\sin\frac{3}{2}\theta)^{-1}\exp[\pm(8\beta/9\alpha)^{1/2}]\cos\frac{3}{2}\theta$ rather than $\exp[-(9\beta/8\alpha)^{1/2}\theta^2]$. It seems wiser, therefore, to try to get better wave functions for evaluating those matrix elements sensitive to this region.

The method used was to adopt the Fourier-series solution—O'Brien's Eq. (23)—and cut off the series when the eigenvectors look sufficiently convergent. The cutoff was chosen at an order such that the last coefficient in the series was $\sim 10^{-6}$ of the first one. As pointed out by O'Brien, the A_u and B_u are 2π periodic Mathieu-type solutions [on replacing 3θ by $2x$, Eq. (1) takes the Mathieu form; the A_u and B_u solutions are each periodic in $\frac{4}{3}\pi$ for θ or 2π for x], so the eigenvalues and Fourier series coefficients published in the N.B.S. tables[33] were used for them. The E_u-type solutions were computed by matrix diagonalization, the requisite order for $\beta/\alpha=36$ being 14×14. The values of 3Γ, c_2, c_3, ϵ, and $E(B_u)-E(A_u)$ so computed are plotted in Fig. 3.

The results for c_3 and 3Γ were found to deviate quite considerably from those indicated by the harmonic-oscillator approximations, e.g., c_3 was higher by a factor of ~ 160 and 3Γ higher by a factor of ~ 8 at $\beta/\alpha=36$, these factors becoming more pronounced as β/α is increased.

APPENDIX D: INTERACTION ENERGY OF COMPLEX WITH LATTICE STRAIN CAUSED BY PHONONS

We assume the host solid to be an isotropic homogeneous continuum with shear modulus β and bulk modulus $\frac{1}{3}(2\alpha+\beta)$.

[33] *Tables Relating to Mathieu Functions* (Columbia University Press, New York, 1951), p. 24.

The energy density due to strain is

$$W=\tfrac{1}{2}\alpha e_{\mu\mu}e_{\nu\nu}+\tfrac{1}{2}\beta e_{\mu\nu}e_{\mu\nu} \tag{D1}$$

(summation over repeated Greek indices). A strain field is accompanied by stresses

$$p_{ij}=\partial W/\partial e_{ij}, \tag{D2}$$

which give the forces necessary to maintain the shape of a hole cut out of the strained solid as

$$F_i=p_{i\mu}dS_\mu$$

on the element of area dS of the area S defining the hole. If the hole is filled by the complex, the complex must push against these forces in order to distort the hole. The extra energy required to do this is then

$$W=\sum_{\text{surface}}\mu_\nu' F_\nu=\int_S u_\nu' p_{\nu\mu}dS_\mu, \tag{D3}$$

where u_i is the component of displacement of surface. When there are no body forces, $p_{ij,j}=0$ and we can write

$$W=\int_V e_{\nu\mu}' p_{\nu\mu}dV$$

$$=\Omega e_{\nu\mu}' p_{\nu\mu}. \tag{D4}$$

Here Ω is the volume of the hole. We are only interested in W for strains like e_{ii} (A_1- and E-type distortions of the octahedron). With this restriction and noting that

$$p_{ii}=\partial W/\partial e_{ii}=\alpha e_{\mu\mu}+\beta e_{ii},$$

we find

$$W=\Omega e_{\nu\nu}'(\alpha e_{\mu\mu}+\beta e_{\nu\nu})$$
$$=\Omega[(3\alpha+\beta)e_{A_1}'e_{A_1}+\beta(e_\theta' e_\theta+e_\epsilon' e_\epsilon)], \tag{D5}$$

where

$$\begin{bmatrix} e_{A_1} \\ e_\theta \\ e_\epsilon \end{bmatrix}=\begin{bmatrix} \sqrt{\frac{1}{3}} & \sqrt{\frac{1}{3}} & \sqrt{\frac{1}{3}} \\ -\sqrt{\frac{1}{6}} & -\sqrt{\frac{1}{6}} & \sqrt{\frac{2}{3}} \\ \sqrt{\frac{1}{2}} & -\sqrt{\frac{1}{2}} & \end{bmatrix}\begin{bmatrix} e_{xx} \\ e_{yy} \\ e_{zz} \end{bmatrix}.$$

Recalling that $\sqrt{2}Re_\theta'=Q_\theta$, $\sqrt{2}Re_\epsilon'=Q_\epsilon$, and that the volume of the octahedron is $\Omega=\frac{4}{3}R^3$, we have

$$\mathcal{H}_c(e)=\tfrac{2}{3}\sqrt{2}R^2\beta(Q_\theta e_\theta+Q_\epsilon e_\epsilon). \tag{D6}$$

β may be related to the density d and velocity of transverse sound, v_T, if desired, by $\beta=dv_T^2$.

It is interesting to compare this result with that obtained by assuming the lattice wave to be uniform throughout the unit cell,[6] so that the simple projection onto the ligands of the complex gives the interaction to be

$$\mathcal{H}_c(e)=\sqrt{2}VR(e_\theta\cos\theta+e_\epsilon\sin\theta). \tag{D7}$$

The radial minimum of the lower-potential sheet occurs at ρ_0 where $\mu\omega^2\rho_0=V$, but $\mu\omega^2$ is just the force constant for the e mode, κ. Thus $\sqrt{2}VR=\sqrt{2}\kappa\rho_0 R$ in (D7). The shear modulus $\beta\approx\kappa'/R$, where κ' is an interatomic elastic constant typical of the crystals and (D6) becomes

$$\mathcal{H}_c(e)=\tfrac{2}{3}\sqrt{2}R\kappa'\rho_0(e_\theta\cos\theta+e_\theta\sin\theta). \tag{D8}$$

The ratio of the two coupling constants is $\frac{3}{2}\kappa/\kappa'$, illustrating directly the dependence on the relative hardness of the complex to that of the crystal.

APPENDIX E: DERIVATION OF RELAXATION TIME BETWEEN TWO GROUPS OF LINES IN INTERNAL THERMAL EQUILIBRIUM

We suppose the levels to be divided into two groups, a and b, each group in internal equilibrium over the time scale for intergroup relaxation. Let the populations be denoted by $n(j,m_j)$, where $m_j=a$ or b, and j refers to levels within the group. If $W(im_i;\,jm_j)$ is the spontaneous transition rate from im_i to jm_j and $N_m=\sum_i n(i,m)$, $m=a,\ b$ then

$$N_a=-\sum_{ij}n(i,a)W(ia;\,jb)+\sum_{ij}n(j,b)W(jb;\,ia); \tag{E1}$$

but

$$n(i,m)=\frac{N_m}{Z_m}\exp\left(-\frac{E(i,m)}{kT}\right),$$

where

$$Z_m=\sum_i\exp\left(-\frac{E(i,m)}{kT}\right)$$

for thermal equilibrium within a group, and

$$\frac{W(jb;\,ia)}{W(ia;\,jb)}=\exp\left(\frac{E(j,b)-E(i,a)}{kT}\right)$$

in general, so that (D7) becomes

$$\frac{dN_a}{dt}=-\sum_{ij}\left[\frac{N_a}{Z_a}\exp\left(-\frac{E(i,a)}{kT}\right)-\frac{N_b}{Z_b}\exp\left(-\frac{E(i,a)}{kT}\right)\right]W(ia;\,jb).$$

Application of the normalization $N_a+N_b=1$ gives a relaxation rate for N_a to equilibrium of

$$\frac{1}{\tau}=\sum_{ij}\left(\frac{1}{Z_a}+\frac{1}{Z_b}\right)\exp\left(-\frac{E(i,a)}{kT}\right)W(ia;\,jb). \tag{E2}$$

On inserting the special form (38) for W, we have

$$\frac{1}{\tau}=\mathfrak{A}\sum_{ij}\left(\frac{1}{Z_a}+\frac{1}{Z_b}\right)u(ia;\,jb)\times\frac{E(i,a)-E(j,b)}{\exp[E(i,a)/kT]-\exp[E(j,b)/kT]}.$$

When $E(i,m)\ll kT$, we have $Z_a\approx Z_b\approx\eta$, the number of levels in each group and the right-hand factor $\rightarrow 1$, giving

$$\frac{1}{\tau}\frac{2}{\eta}=-\mathfrak{A}kT\sum_{ij}u(ia;\,jb). \tag{E3}$$

Since the groups are in thermal equilibrium, the magnetization for a given distortion is linearly related (independent of time) to N_a, so that the magnetization of each distortion has the same relaxation given by (E3).

PHYSICAL REVIEW VOLUME 179, NUMBER 2 10 MARCH 1969

Systematics of the Hyperfine and Exchange Interactions in the Chromium Chalcogenide Spinels

S. B. BERGER*
RCA Laboratories, Princeton, New Jersey 08540
AND
J. I. BUDNICK AND T. J. BURCH
Fordham University,† Bronx, New York 10458
(Received 10 June 1968)

The NMR of nuclei at each site in the cadmium and mercury chromium chalcogenide spinels has been studied at 1.4°K. Experimentally, we find an approximately linear relation between the isotropic hyperfine field of ^{53}Cr nuclei and the near-neighbor chromium-chromium exchange constants. This observation is interpreted in terms of a systematic variation in covalency and constant overlap for these compounds. The ^{77}Se isotropic hyperfine field is large and oppositely directed to the magnetization. This field can be understood in terms of a spin polarization of Se s orbitals by the unpaired Cr spins. The Cr and Se results are consistent with a theoretical formulation due to Huang and Orbach. The ^{199}Hg, ^{201}Hg, ^{111}Cd, and ^{113}Cd hyperfine fields are found to be isotropic, large, and positive with respect to the magnetization. These fields are shown to be mainly due to overlap of unfilled outer s shells of these nonmagnetic ions with the Cr $3d$ orbits.

THE magnetic chromium chalcogenide spinels offer an unique opportunity to study the hyperfine interactions of nuclei in a system for which the relevant exchange interactions have been independently determined.[1] We have investigated the NMR of all nuclei except sulfur in $CdCr_2S_4$, $CdCr_2Se_4$, $HgCr_2S_4$, and $HgCr_2Se_4$. The similar angular relationship of the cations to the anions in these compounds is reflected by their identical crystallographic u parameters.[1] This factor, the essentially constant ionic radii,[1] and the direct correlation of our NMR data to the nearest-neighbor (nn) exchange parameter allow reliable conclusions concerning covalency and overlap to be drawn for this system.[2]

In this paper we report new NMR data for these compounds from which we conclude: (1) the ^{53}Cr isotropic hyperfine interaction exhibits an approximately linear variation with the nn exchange interaction, and (2) the nonmagnetic cation (Cd or Hg) hyperfine interaction and the next nearest-neighbor (nnn) chromium exchange interaction[1] are dominated by an overlap contribution, since both are noted to decrease with increasing lattice parameter. The first observation differs from that found for the dissimilar manganese monochalcogenide series[3] and is describable as a systematic variation of the covalency in the present compounds consistent with a theoretical evaluation of the important nn exchange paths.[4] This covalency change is also a critical part of our interpretation of the Se hyperfine interactions.

In Table I, a summary of our results for the isotropic hyperfine fields H_{iso} in these compounds is presented. The data were obtained at 1.4°K using spin-echo techniques on polycrystalline samples. For the noncubic sites the spectra were analyzed to determine the isotropic contribution.[5,6] The signs were found by measuring the frequency shift upon application of a magnetic

* Jointly sponsored by Air Force Cambridge Research Laboratories, Office of Aerospace Research, under Contract F19628-67-C0175, and RCA Laboratories, Princeton, New Jersey, but this report does not necessarily reflect endorsement by the sponsor.
† Supported in part by the National Science Foundation.

[1] P. K. Baltzer, P. J. Wojtowicz, M. Robbins, and E. Lopatin, Phys. Rev. **151**, 367 (1966).
[2] R. E. Watson and A. J. Freeman, in *Hyperfine Interactions* edited by A. J. Freeman and R. B. Frankel (Academic Press Inc., New York, 1967), pp. 81–91.
[3] E. D. Jones, Phys. Rev. **151**, 315 (1966).
[4] Nai L. Huang and R. Orbach, J. Appl. Phys. **39**, 426 (1968).
[5] S. B. Berger, J. I. Budnick, and T. J. Burch, J. Appl. Phys. **39**, 658 (1968).
[6] G. H. Stauss, M. Rubinstein, J. Feinleib, K. Dwight, N. Menyuk, and A. Wold, J. Appl. Phys. **39**, 667 (1968).